Children Orthotics and Prostheses Devices Designed from Cinematic and Dynamic Considerations

C. Copilusi, N. Dumitru, M. Marin and L. Rusu

***Abstract*— A study concerning the children locomotion system is presented through this research. The research aim is to obtain the motion laws developed by the children locomotion system's articulations and connection forces which are produced in their structure in the walking activity. These parameters are useful for orthotic and prosthetic systems design for children with ages between 4-7 years. The study is based on an experimental analysis developed with ultra high-speed video equipment on 20 children. From the experimental analysis significant data will be used for a human locomotion system cinematic analysis. With these, a dynamic analysis will be performed on analytical way in order to obtain the connection forces from the human locomotion system joints. Data obtained from cinematic and dynamic analyses represents the input parameters for designing a modular knee orthosis mechanism and a parameterized knee prosthesis mechanical system which uses a cam mechanism in his structure.**

***Index Terms*— cinematic, dynamics, locomotion system, orthotics, prosthesis**

I. Introduction

THE main motivation for these analyses was given by the prosthesis and orthotics devices development restriction for children. It is known that the restriction is imposed by the fact that children are in growth continuously especially between 4-7 years. Due to this fact modular orthotics devices and parameterized prosthetics can be developed in order to improve the locomotion system and to satisfy the ability to move. For this it is necessary to perform experimental, analytical, and design analyses in order to create databases useful in this research direction. It can be mentioned similar research work in this field by [24], [3], [16], [17], [12], [15] and [11]. Similar dynamic analyses with remarkable result can be found in [2], [16], [18], and [27]. The research main aim was to obtain the connection forces from each human locomotion system articulation when the healthy subject will perform the walking activity. This will serve as input data for dynamic analysis developed on analytical way.

Manuscript received October 9, 2012. The research work reported here was made possible by Grant CNCSIS –UEFISCSU, project number PNII – RU – PD – 2009 – 1 code: 55/28.07.2010.

C. Copilusi is with the Faculty of Mechanics, University of Craiova. Calea Bucuresti street no. 107. Romania (corresponding author to provide phone: +04 0747222771; e-mail: cristache03@yahoo.co.uk).

N. Dumitru is with Faculty of Mechanics, University of Craiova. Calea Bucuresti street no. 113. Romania (e-mail: dumitru_nic2011@yahoo.com).

M. Marin is with Faculty of Mechanics, University of Craiova. Calea Bucuresti street no. 113. Romania (e-mail: mih_marin@yahoo.com).

L. Rusu is with Faculty of Educational Physics and Sports, University of Craiova. Brestei street. Romania. (e-mail:rusuligia@gmail.com).

II. Experimental Research

Taking into account the experimental research aim, the motions developed by the human locomotion system [2], [27], [5], [6], [7] presented here will be evaluated experimentally by using motion analysis equipment, which is called CONTEMPLAS. This has two high speed cameras for capturing and recording sequences and a DELL notebook for sequences analysis in real time with Templo Standard module software [13]. The University of Craiova-Faculty of Mechanics owns this special equipment, which is used for the experimental research. This equipment enables us to determine the desired points trajectories and spatial angular variations onto either mechanical or biomechanical mobile systems through successive identifications of the joint centers positions in their structures. The general procedure for experimental determinations is shown in Fig. 1.

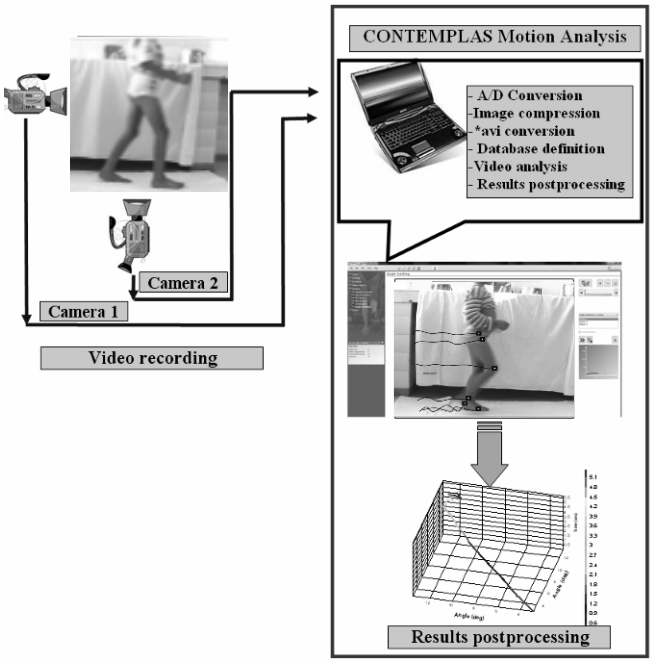

Fig. 1. CONTEMPLAS Motion equipment and analysis scheme

Thus, one attached markers in the rotation joints centers with a view to determining the angular amplitude developed by the human locomotion system. A sequence of the

experimental analysis using this equipment is shown in Fig. 2, Fig. 3, Fig. 4 and Fig. 5. In this sequence children have to perform 3 steps for walking activity. For this experimental research a number of 20 children with ages between 4-7 years were used. Markers have been attached on human locomotion system's articulations centers, in order to determine trajectories and angular amplitudes. These motion laws forms a database which consists in a number of 4 segments, each segment consists in 5 healthy children with the same age.

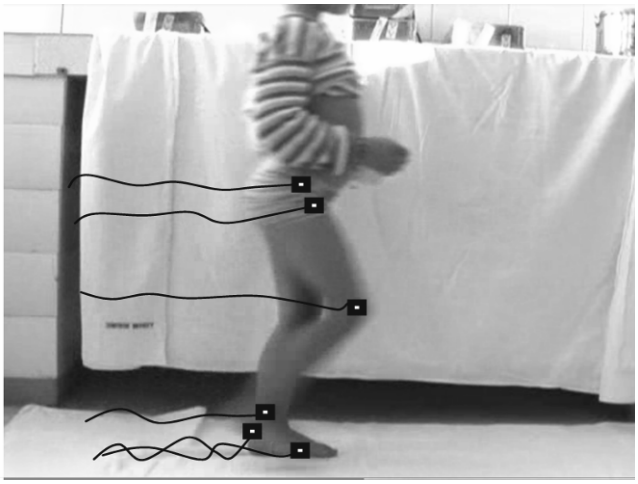

Fig. 2. Experimental analysis sequence for joints trajectories (4 years old child case)

Fig. 3. Experimental analysis sequence for hip joint angular amplitude

Also the height interval for all the analyzed children was: 95-136 cm. Weight of these subjects was between 21-36 kilograms. In each segment was 1 girl and the rest of the subjects were boys. The cameras record simultaneously the markers trajectories and angular amplitudes for each lower limb. As an example of the final results, one presents the motion laws for the analyzed articulations in diagrams from Fig. 6, Fig.7, Fig.8 and Fig.9.

Fig. 4. Experimental analysis sequence for knee joint angular amplitude

Fig. 5. Experimental analysis sequence for ankle joint angular amplitude

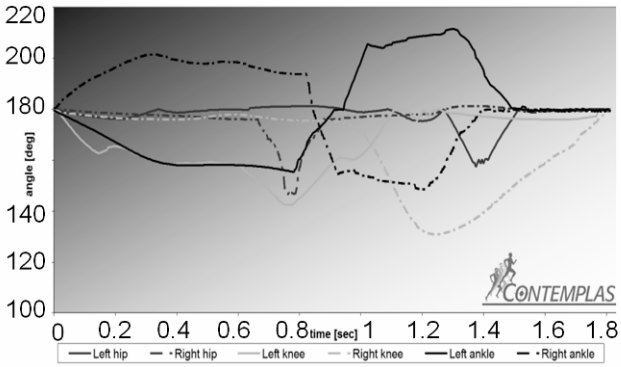

Fig. 6. Locomotion system's angular amplitudes average for children at 4 years for walking activity

The angular amplitude of each joint is a functional angle for lower limb joints, means useful angle for develops movement from ADL scale (activity daily living scale) present by the trajectories of the joints. The average angular amplitudes during the gait cycle on the examined children segments are presented in Table 1, where: IC-Initial Contact, LR-Loading Response, MSt-MidStance, TSt-Terminal Stance, PSw-PreSwing, ISw-Initial Swing, MSw-MidSwing, TSw-Terminal Swing.

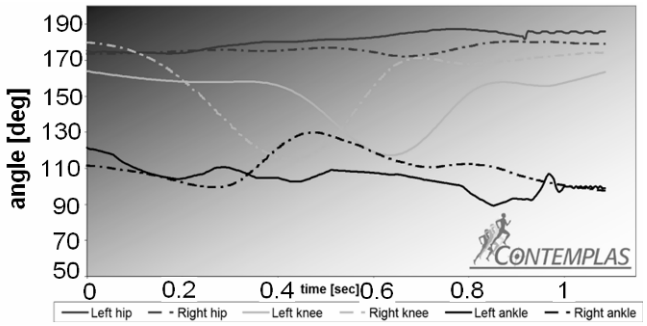

Fig. 7. Locomotion system's angular amplitudes average for children at 5 years for walking activity

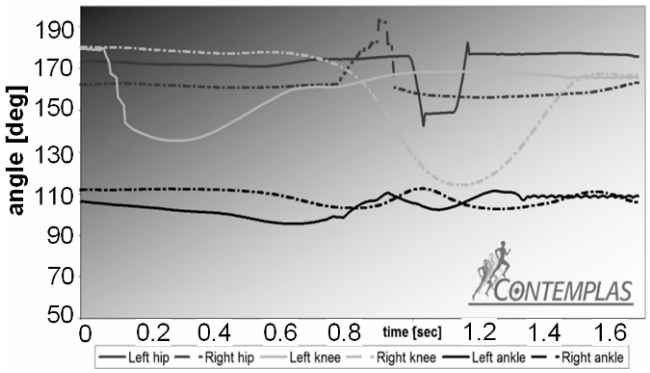

Fig. 8. Locomotion system's angular amplitudes average for children at 6 years for walking activity

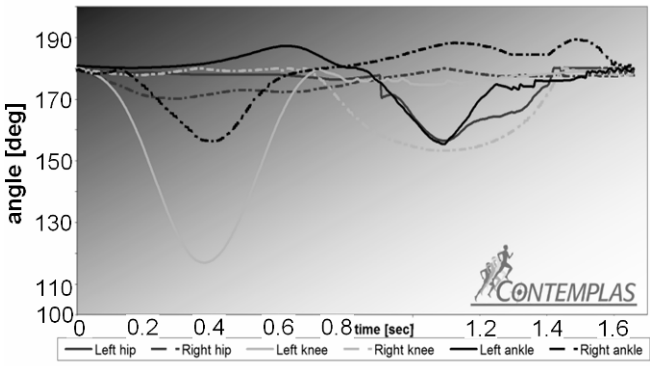

Fig. 9. Locomotion system's angular amplitudes average for children at 7 years for walking activity

TABLE I
AVERAGE ANGULAR AMPLITUDES FROM ANALYZED HUMAN SUBJECTS

Joints / Gait phase	Segment 1 with 4 years age			Segment 2 with 5 years		
	Hip	**Knee**	**Ankle**	**Hip**	**Knee**	**Ankle**
IC	**19.71°**	**4.23°**	**-6.51°**	**19.85°**	**4.78°**	**-6.56°**
LR	**14.08°**	**13.76°**	**-15.48°**	**14°**	**13.82°**	**-15.9°**
Mst	**-14.5°**	**0.87°**	**-5.37°**	**-15.62°**	**1.02°**	**-5.42°**
Tst	**-22.7°**	**3.08°**	**-2.17°**	**-23.01°**	**5.23°**	**-1.95°**
PSw	**-16.4°**	**39.35°**	**27.39°**	**-16.51°**	**40.02°**	**27.44°**
ISw	**10.9°**	**53.68°**	**14.29°**	**10.93°**	**52.16°**	**14.44°**
MSw	**17.01°**	**15.08°**	**11.78°**	**16.98°**	**15.59°**	**12.35°**
TSw	**16.17°**	**7.83°**	**10.21°**	**16.23°**	**6.42°**	**11.52°**
	Segment 3 with 6 years age			**Segment 4 with 7 years age**		
IC	**19.98°**	**5.23°**	**-7.03°**	**20.36°**	**6.36°**	**-10.5°**
LR	**14.52°**	**14.11°**	**-16.35°**	**15.87°**	**15.99°**	**-18.9°**
Mst	**-14.9°**	**1.12°**	**-5.98°**	**-16.64°**	**0.52°**	**-7.36°**
Tst	**-23.2°**	**6.49°**	**-0.87°**	**-25.61°**	**7.83°**	**0.12°**
PSw	**-17.5°**	**42.23°**	**28.39°**	**-19.22°**	**46.29°**	**30.21°**
ISw	**11.01°**	**54.63°**	**15.92°**	**12.21°**	**55.31°**	**16.05°**
MSw	**17.23°**	**16.32°**	**13.62°**	**18.34°**	**17.58°**	**14.21°**
TSw	**16.69°**	**8.42°**	**12.96°**	**18.48°**	**9.13°**	**13.62°**

III. HUMAN LOCOMOTION SYSTEM CINEMATIC ANALYSIS

The method used here has a flexible character and assures an interface for dynamic analysis especially for finite element modeling of spatial and planar mobile mechanical systems [5], [10], [12], [15], [16], [17] and [18]. The general method is presented bellow.

For obtaining the general mathematic model it will be considered a cinematic element realized from n solid rigid bodies connected together through n-1 cinematic pairs (Fig. 10).

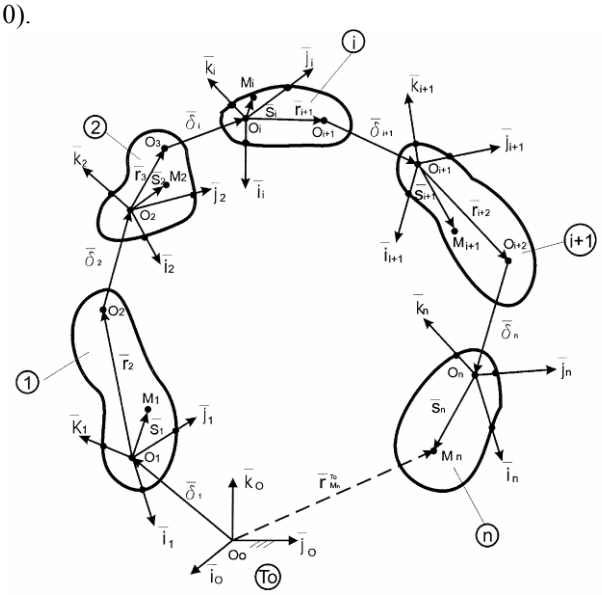

Fig.10. Cinematic element realized from n solid rigid bodies connected together through n-1 cinematic pairs

For this cinematic element we make the following notations: $T_i(x_i, y_i, z_i)$, represents the reference coordinate system attached to **i** element, having the $\overline{W_i}(\overline{i_i}, \overline{j_i}, \overline{k_i})$, versors base with $i = \overline{1,n}$; $T_0(x_0, y_0, z_0)$, represents the global reference system with $\overline{W_0}(\overline{i_0}, \overline{j_0}, \overline{k_0})$ versors base; $\overline{\delta_i}$, represents the relative translation vector between *i-1* and **i** elements, depending with T_{i-1} tried, if exists a translation joint between *i-1* and *i*, ($i = \overline{1,n}$); $\overline{r_i}$, represents the position vector which depends with T_{i-1}, reference system, against with O_I', point, when the relative translation starts ($i = \overline{1,n}$); $\overline{S_i}$ represent the position vector of the M_i, depending with T_i, attached to *i* element.

For determine the position vector of M_n point, in rapport with the global reference system is given by the relation:

$$\overline{r}_{Mn}^{T0} = \overline{O_0 M_n} = \sum_{i=1}^{n} \left(\overline{r_i} + \overline{\delta_i}\right) + \overline{S_n} \tag{1}$$

Where:

$$\overline{r_i} = \left\{r_i^x, r_i^y, r_i^z\right\}^T{}_{i-1} = \left\{r_i\right\}^T \left\{\overline{W}_{i-1}\right\} \tag{2}$$

$$\overline{\delta_i} = \left\{\delta_i^x, \delta_i^y, \delta_i^z\right\}^T{}_{i-1} = \left\{\delta_i\right\}^T \left\{\overline{W}_{i-1}\right\} \tag{3}$$

$$\overline{S_n} = \left\{S_n^x, S_n^y, S_n^z\right\}^T{}_{i-1} = \left\{S_n\right\}^T \left\{\overline{W}_n\right\} \tag{4}$$

We introduce the transformation coordinates matrix, for crossing from a reference coordinate system to another:

$$\left\{\overline{W}_{i-1}\right\} = \left[A_{0,i-1}\right] \cdot \left\{\overline{W}_0\right\} \tag{5}$$

We consider the following connection order:

0 – 1 – 2 – 3 – .... – i-1 – i ...n

The (2), (3) and (4) relation will be:

$$\overline{r_i} = \left\{r_i\right\}^T \left\{\overline{W}_{i-1}\right\} = \left\{r_i\right\}^T \left[A_{0,i-1}\right] \left\{\overline{W}_0\right\} \tag{6}$$

$$\overline{\delta_i} = \left\{\delta_i\right\}^T \left\{\overline{W}_{i-1}\right\} = \left\{\delta_i\right\}^T \left[A_{0,i-1}\right] \left\{\overline{W}_0\right\} \tag{7}$$

$$\overline{S_n} = \left\{S_n\right\}^T \left\{\overline{W}_{i-1}\right\} = \left\{S_n\right\}^T \left[A_{0,n}\right] \left\{\overline{W}_0\right\} \tag{8}$$

By introducing the (6), (7), (8) in (1), we obtain:

$$\overline{r}^{T0}_{Mn} = \overline{O_0 M_n} = \sum_{i=1}^{n} \left(\begin{pmatrix} \left\{r_i\right\}^T + \left\{\delta_i\right\}^T \cdot \left[A_{0,i-1}\right] + \\ + \left\{S_n\right\}^T \cdot \left[A_{0,n}\right] \end{pmatrix} \right) \cdot \left\{\overline{W}_0\right\} \tag{9}$$

The speed calculus will be obtained by differentiating the (9) depending on time. Considering the coordinates transformation matrix as a quadratic one, the following relation will be written:

$$\left[A_{0i}\right] \cdot \left[A_{0i}\right]^T = \left[I\right] \tag{10}$$

By differentiating the (10) relation in rapport with time, we obtain:

$$\left[\dot{A}_{0i}\right] \cdot \left[A_{0i}\right]^T + \left[A_{0i}\right] \cdot \left[\dot{A}_{0i}\right]^T = 0 \tag{11}$$

$$\left[\left[\dot{A}_{0i}\right] \cdot \left[A_{0i}^T\right]\right]^T = \left[A_{0i}\right] \cdot \left[\dot{A}_{0i}\right]^T = -\left[\dot{A}_{0i}\right] \cdot \left[A_{0i}\right]^T \tag{12}$$

We observe that $\left[\dot{A}_{0i}\right] \cdot \left[A_{0i}\right]^T$ - term is an non symmetric matrix:

$$\left[\tilde{\omega}_{0i}\right] = \left[\dot{A}_{0i}\right] \cdot \left[A_{0i}\right]^T \tag{13}$$

By multiplying the (13) relation with $\left[A_{0i}\right]$, it will obtain:

$$\left[\tilde{\omega}_{0i}\right] \cdot \left[A_{0i}\right] = \left[\dot{A}_{0i}\right] \tag{14}$$

Differentiating (9) relation in rapport with time, we obtain:

$$\dot{\overline{r}}^{T0}_{M0} = \sum_{i=1}^{n} \left(\begin{pmatrix} \left\{r_i\right\}^T \cdot \left[\tilde{\omega}_{0,i-1}\right] + \left\{\dot{\delta}_i\right\}^T + \\ + \left\{\delta_i\right\}^T \cdot \left[\tilde{\omega}_{0,i-1}\right] \end{pmatrix} \cdot \left[A_{0,i-1}\right] + \right. \\ \left. + \left\{S_n\right\}^T \cdot \left[\tilde{\omega}_{0n}\right] \cdot \left[A_{0,n}\right] \right) \cdot \left\{\overline{W}_0\right\} \tag{15}$$

We obtain the following non symmetric matrix:

$$\left[\tilde{\omega}_{0,p}\right] = \begin{bmatrix} 0 & \omega_{0p}^z & -\omega_{0p}^y \\ -\omega_{0p}^z & 0 & \omega_{0p}^x \\ \omega_{0p}^y & -\omega_{0p}^x & 0 \end{bmatrix} \tag{16}$$

Where:

$$\overline{\omega}_{0,p} = \omega_{0,p}^x \overline{i} + \omega_{0,p}^y \overline{j} + \omega_{0,p}^z \overline{k} \tag{17}$$

For each vector $\overline{\delta_i}$, $\overline{r_i}$ and $\overline{S_i}$, ($i = \overline{1,n}$), a non symmetric matrix can be attached, as has been done in (16). The used terms in (15), in the following form can be written:

$$\left\{r_i\right\}^T \left[\tilde{\omega}_{0,i-1}\right] = \left\{\omega_{0,i-1}\right\}^T \left[\tilde{r}_i\right] \tag{18}$$

$$\left\{\delta_i\right\}^T \left[\tilde{\omega}_{0,i-1}\right] = \left\{\omega_{0,i-1}\right\}^T \left[\tilde{\delta}_i\right] \tag{19}$$

$$\left\{S_n\right\}^T \left[\tilde{\omega}_{0,n}\right] = \left\{\omega_{0,n}\right\}^T \left[\tilde{S}_n\right] \tag{20}$$

$$\left\{\omega_{op}\right\} = \left\{\omega_p^x, \omega_p^y, \omega_p^z\right\} \tag{21}$$

In this case, the (15) relation can be written:

$$\overline{V}^{T0}_{Mn} = \left(\begin{pmatrix} \sum_{i=1}^{n} \left(\left\{\omega_{0,i-1}\right\}^T \left[\tilde{r}_i\right] + \right. \right. \\ \left. + \left\{\omega_{0,i-1}\right\}^T \left[\tilde{\delta}_i\right] \right) \cdot \left[A_{0,i-1}\right] + \\ + \sum_{i=1}^{n} \left[A_{0,i-1}\right]^T \left[\dot{\tilde{\delta}}_i\right] + \\ \left. + \left\{\omega_{0,n}\right\}^T \left[\tilde{S}_n\right] \cdot \left[A_{0,n}\right] \end{pmatrix} \right) \cdot \left\{\overline{W}_0\right\} = \\ = \left(\begin{pmatrix} \sum_{i=1}^{n} \left(\left\{\omega_{0,i-1}\right\}^T \left[\tilde{r}_i\right] \cdot \left[A_{0,i-1}\right] + \right. \\ + \sum \left\{\dot{\tilde{\delta}}_i\right\}^T \cdot \left[A_{0,i-1}\right] + \\ \left. + \sum_{i=1}^{n} \left\{\omega_{0,i-1}\right\}^T \left[\tilde{\delta}_i\right] \cdot \left[A_{0,i-1}\right] + \right. \\ \left. + \left\{\omega_{0,n}\right\}^T \left[\tilde{S}_n\right] \cdot \left[A_{0,n}\right] \end{pmatrix} \right) \cdot \left\{\overline{W}_0\right\} \tag{22}$$

For the acceleration calculus it can be obtained by differentiating the (22) depending on time.

For this analysis the cinematic model presented in Fig. 10, will be considered. The cinematic analysis will be performed for walking; only one gait when a foot is fixed with the ground and the other perform the desired motion. The cinematic parameters variation laws were obtained by processing with the MAPLE software aid the mathematical models which are defining the human locomotion system experimentally cinematic analysis.

From a structural viewpoint, the cinematic chain it consists in 16 rotation joints. The $\overrightarrow{r_R^{OT}}$ vector, has the following expression:

$$\begin{aligned}\overrightarrow{r_R^{OT}} = {} & \vec{r}_1 + \vec{r}_2 + \vec{r}_3 + \vec{r}_4 + \vec{r}_5 + \vec{r}_6 + \vec{r}_7 + \vec{r}_8 + \vec{r}_9 + \\ & + \vec{r}_{10} + \vec{r}_{11} + \vec{r}_{12} + \vec{r}_{13} + \vec{r}_{14} + \vec{r}_{15} + \vec{r}_{16} + \vec{S}_{17}\end{aligned} \tag{23}$$

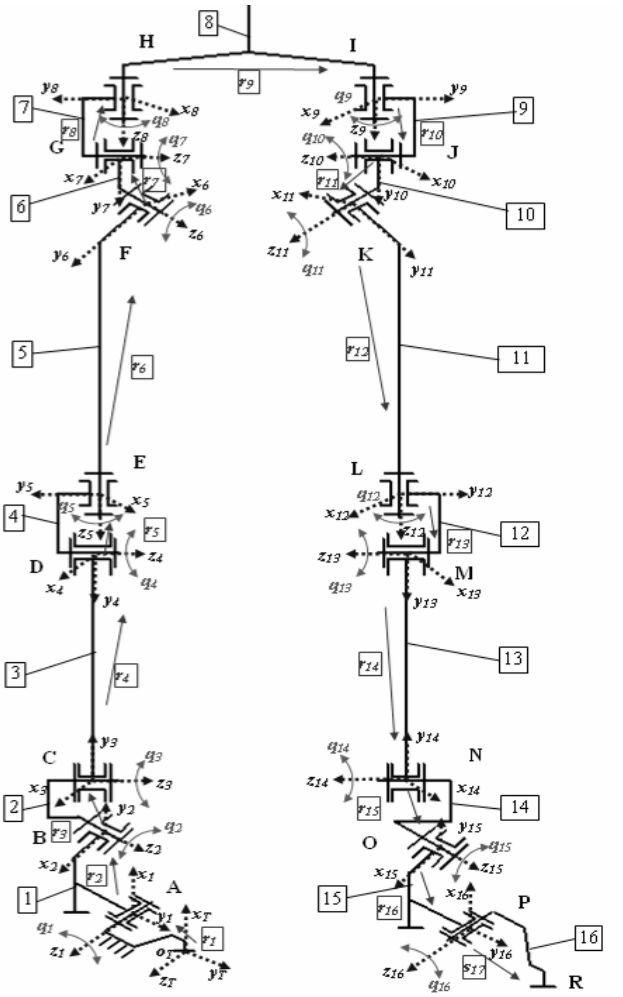

Fig. 10. Human locomotion system cinematic model

The connectivity order will be: OT – 1 – 2 – 3 – 4 – 5 – 6 – 7 – 8– 9 – 10 – 11 – 12 – 13 – 14 – 15 – 16.

A. Position calculus

The position vectors are given by relation (24).

Changing the versors base at crossing from a reference coordinate system to another (introducing the coordinate transformation matrices), one the relation (25) to (41) it will be obtained.

$$\begin{aligned}
\overrightarrow{r_1} &= \{r_1^x, r_1^y, r_1^z\} = \{r_1\}^T \cdot \{\overrightarrow{W_{OT}}\} \\
\overrightarrow{r_2} &= \{r_2^x, r_2^y, r_2^z\} = \{r_2\}^T \cdot \{\overrightarrow{W_1}\} \\
\overrightarrow{r_3} &= \{r_3^x, r_3^y, r_3^z\} = \{r_3\}^T \cdot \{\overrightarrow{W_2}\} \\
\overrightarrow{r_4} &= \{r_4^x, r_4^y, r_4^z\} = \{r_4\}^T \cdot \{\overrightarrow{W_3}\} \\
\overrightarrow{r_5} &= \{r_5^x, r_5^y, r_5^z\} = \{r_5\}^T \cdot \{\overrightarrow{W_4}\} \\
\overrightarrow{r_6} &= \{r_6^x, r_6^y, r_6^z\} = \{r_6\}^T \cdot \{\overrightarrow{W_5}\} \\
\overrightarrow{r_7} &= \{r_7^x, r_7^y, r_7^z\} = \{r_7\}^T \cdot \{\overrightarrow{W_8}\} \\
\overrightarrow{r_8} &= \{r_8^x, r_8^y, r_8^z\} = \{r_8\}^T \cdot \{\overrightarrow{W_7}\} \\
\overrightarrow{r_9} &= \{r_9^x, r_9^y, r_9^z\} = \{r_9\}^T \cdot \{\overrightarrow{W_8}\} \\
\overrightarrow{r_{10}} &= \{r_{10}^x, r_{10}^y, r_{10}^z\} = \{r_{10}\}^T \cdot \{\overrightarrow{W_9}\} \\
\overrightarrow{r_{11}} &= \{r_{11}^x, r_{11}^y, r_{11}^z\} = \{r_{11}\}^T \cdot \{\overrightarrow{W_{10}}\} \\
\overrightarrow{r_{12}} &= \{r_{12}^x, r_{12}^y, r_{12}^z\} = \{r_{12}\}^T \cdot \{\overrightarrow{W_{11}}\} \\
\overrightarrow{r_{13}} &= \{r_{13}^x, r_{13}^y, r_{13}^z\} = \{r_{13}\}^T \cdot \{\overrightarrow{W_{12}}\} \\
\overrightarrow{r_{14}} &= \{r_{14}^x, r_{14}^y, r_{14}^z\} = \{r_{14}\}^T \cdot \{\overrightarrow{W_{13}}\} \\
\overrightarrow{r_{15}} &= \{r_{15}^x, r_{15}^y, r_{15}^z\} = \{r_{15}\}^T \cdot \{\overrightarrow{W_{14}}\} \\
\overrightarrow{r_{16}} &= \{r_{16}^x, r_{16}^y, r_{16}^z\} = \{r_{16}\}^T \cdot \{\overrightarrow{W_{15}}\} \\
\overrightarrow{S_{17}} &= \{S_{17}^x, S_{17}^y, S_{17}^z\} = \{S_{17}\}^T \cdot \{\overrightarrow{W_{16}}\}
\end{aligned} \tag{24}$$

$$\{\overline{W_1}\} = [A_{OT1}] \cdot \{\overline{W_{OT}}\}; \tag{25}$$

$$\{\overline{W_2}\} = [A_{12}] \cdot \{\overline{W_1}\} = [A_{OT2}] \cdot \{\overline{W_{OT}}\}; \tag{26}$$

$$\{\overline{W_3}\} = [A_{23}] \cdot \{\overline{W_2}\} = [A_{OT3}] \cdot \{\overline{W_{OT}}\}; \tag{27}$$

$$\{\overline{W_4}\} = [A_{34}] \cdot \{\overline{W_3}\} = [A_{OT4}] \cdot \{\overline{W_{OT}}\}; \tag{28}$$

$$\{\overline{W_5}\} = [A_{45}] \cdot \{\overline{W_4}\} = [A_{OT5}] \cdot \{\overline{W_{OT}}\}; \tag{29}$$

$$\{\overline{W_6}\} = [A_{56}] \cdot \{\overline{W_5}\} = [A_{OT6}] \cdot \{\overline{W_{OT}}\}; \tag{30}$$

$$\{\overline{W_7}\} = [A_{67}] \cdot \{\overline{W_6}\} = [A_{OT7}] \cdot \{\overline{W_{OT}}\}; \tag{31}$$

$$\{\overline{W_8}\} = [A_{78}] \cdot \{\overline{W_7}\} = [A_{OT8}] \cdot \{\overline{W_{OT}}\}; \tag{32}$$

$$\{\overline{W_9}\} = [A_{89}] \cdot \{\overline{W_8}\} = [A_{OT9}] \cdot \{\overline{W_{OT}}\}; \tag{33}$$

$$\{\overline{W_{10}}\} = [A_{910}] \cdot \{\overline{W_9}\} = [A_{OT10}] \cdot \{\overline{W_{OT}}\}; \tag{34}$$

$$\{\overline{W_{11}}\} = [A_{1011}] \cdot \{\overline{W_{10}}\} = [A_{OT11}] \cdot \{\overline{W_{OT}}\}; \tag{35}$$

$$\{\overline{W_{12}}\} = [A_{1112}] \cdot \{\overline{W_{11}}\} = [A_{OT12}] \cdot \{\overline{W_{OT}}\}; \tag{36}$$

$$\{\overline{W_{13}}\} = [A_{1213}] \cdot \{\overline{W_{12}}\} = [A_{OT13}] \cdot \{\overline{W_{OT}}\}; \tag{37}$$

$$\{\overline{W_{14}}\} = [A_{1314}] \cdot \{\overline{W_{13}}\} = [A_{OT14}] \cdot \{\overline{W_{OT}}\}; \tag{38}$$

$$\{\overline{W_{15}}\} = [A_{1415}] \cdot \{\overline{W_{14}}\} = [A_{OT15}] \cdot \{\overline{W_{OT}}\}; \tag{39}$$

$$\{\overline{W_{16}}\} = [A_{1516}] \cdot \{\overline{W_{15}}\} = [A_{OT16}] \cdot \{\overline{W_{OT}}\}; \tag{40}$$

$$\{\overline{W_{17}}\} = [A_{1617}] \cdot \{\overline{W_{16}}\} = [A_{OT17}] \cdot \{\overline{W_{OT}}\} \tag{41}$$

By analyzing 25) to (41) we observe that:

$$\begin{aligned}
&[A_{OT2}] = [A_{12}] \cdot [A_{OT}]; \quad [A_{OT3}] = [A_{23}] \cdot [A_{OT1}]; \\
&[A_{OT4}] = [A_{34}] \cdot [A_{OT3}]; \quad [A_{OT5}] = [A_{45}] \cdot [A_{OT4}]; \\
&[A_{OT6}] = [A_{56}] \cdot [A_{OT5}]; \quad [A_{OT7}] = [A_{67}] \cdot [A_{OT6}]; \\
&[A_{OT8}] = [A_{78}] \cdot [A_{OT7}]; \quad [A_{OT9}] = [A_{89}] \cdot [A_{OT8}]; \\
&[A_{OT10}] = [A_{910}] \cdot [A_{OT9}]; \quad [A_{OT11}] = [A_{1011}] \cdot [A_{OT10}]; \\
&[A_{OT12}] = [A_{1112}] \cdot [A_{OT11}]; \quad [A_{OT13}] = [A_{1213}] \cdot [A_{OT12}]; \\
&[A_{OT14}] = [A_{1314}] \cdot [A_{OT13}]; \quad [A_{OT14}] = [A_{1415}] \cdot [A_{OT13}]; \\
&[A_{OT15}] = [A_{1516}] \cdot [A_{OT14}]; \quad [A_{OT16}] = [A_{1617}] \cdot [A_{OT15}].
\end{aligned} \tag{42}$$

Based on (42) we identify the coordinates transformation matrices for each cinematic joints, with $\alpha_{i,i+1}=90^{\circ}$, and $i=\overline{1,16}$. Point: *A, B, C, D, E, F, G, H, I, J, K, L, M, N, O, P* and *R* positions in rapport with T_{OT} coordinate system, bounded to the left foot, will be identified through the (43) to (50). Similarly, we obtain the displacements of other joint centre points. The displacement for *R* point is given by (51).

$$\left\{\overline{r_A^{O_T}}\right\}=\{r_1\}^T\cdot\left\{\overline{W}_{OT}\right\}; \tag{43}$$

$$\left\{\overline{r_B^{O_T}}\right\}=\{r_1\}^T\cdot\left\{\overline{W}_{OT}\right\}+\{r_2\}^T\cdot[A_{OT1}]\cdot\left\{\overline{W}_{OT}\right\}; \tag{44}$$

$$\left\{\overline{r_C^{OT}}\right\}=\{r_1\}^T\cdot\left\{\overline{W}_{OT}\right\}+\{r_2\}^T\cdot[A_{OT1}]\cdot\left\{\overline{W}_{OT}\right\}+ \tag{45}$$
$$+\{r_3\}^T\cdot[A_{12}]\cdot[A_{OT1}]\cdot\left\{\overline{W}_{OT}\right\};$$

$$\left\{\overline{r_D^{OT}}\right\}=\{r_1\}^T\cdot\left\{\overline{W}_{OT}\right\}+\{r_2\}^T\cdot[A_{OT1}]\cdot\left\{\overline{W}_{OT}\right\}+ \tag{46}$$
$$+\{r_3\}^T\cdot[A_{12}]\cdot[A_{OT1}]\cdot\left\{\overline{W}_{OT}\right\}+\{r_4\}^T\cdot[A_{23}]\cdot[A_{12}]\cdot[A_{OT1}]\cdot\left\{\overline{W}_{OT}\right\};$$

$$\left\{\overline{r_E^{OT}}\right\}=\{r_1\}^T\cdot\left\{\overline{W}_{OT}\right\}+\{r_2\}^T\cdot[A_{OT1}]\cdot\left\{\overline{W}_{OT}\right\}+$$
$$+\{r_3\}^T\cdot[A_{12}]\cdot[A_{OT1}]\cdot\left\{\overline{W}_{OT}\right\}+\{r_4\}^T\cdot[A_{23}]\cdot[A_{12}]\cdot[A_{OT1}]\cdot\left\{\overline{W}_{OT}\right\}+ \tag{47}$$
$$+\{r_5\}^T\cdot[A_{34}]\cdot[A_{23}]\cdot[A_{12}]\cdot[A_{OT1}]\cdot\left\{\overline{W}_{OT}\right\};$$

$$\left\{\overline{r_F^{OT}}\right\}=\{r_1\}^T\cdot\left\{\overline{W}_{OT}\right\}+\{r_2\}^T\cdot[A_{OT1}]\cdot\left\{\overline{W}_{OT}\right\}+$$
$$+\{r_3\}^T\cdot[A_{12}]\cdot[A_{OT1}]\cdot\left\{\overline{W}_{OT}\right\}+\{r_4\}^T\cdot[A_{23}]\cdot[A_{12}]\cdot \tag{48}$$
$$\cdot[A_{OT1}]\cdot\left\{\overline{W}_{OT}\right\}+\{r_5\}^T\cdot[A_{34}]\cdot[A_{23}]\cdot[A_{12}]\cdot[A_{OT1}]\cdot$$
$$\cdot\left\{\overline{W}_{OT}\right\}+\{r_6\}^T\cdot[A_{45}]\cdot[A_{34}]\cdot[A_{23}]\cdot[A_{12}]\cdot[A_{OT1}]\cdot\left\{\overline{W}_{OT}\right\};$$

$$\left\{\overline{r_G^{OT}}\right\}=\{r_1\}^T\cdot\left\{\overline{W}_{OT}\right\}+\{r_2\}^T\cdot[A_{OT1}]\cdot\left\{\overline{W}_{OT}\right\}+$$
$$+\{r_3\}^T\cdot[A_{12}]\cdot[A_{OT1}]\cdot\left\{\overline{W}_{OT}\right\}+\{r_4\}^T\cdot[A_{23}]\cdot[A_{12}]\cdot$$
$$\cdot[A_{OT1}]\cdot\left\{\overline{W}_{OT}\right\}+\{r_5\}^T\cdot[A_{34}]\cdot[A_{23}]\cdot[A_{12}]\cdot[A_{OT1}]\cdot\left\{\overline{W}_{OT}\right\}+ \tag{49}$$
$$+\{r_6\}^T\cdot[A_{45}]\cdot[A_{34}]\cdot[A_{23}]\cdot[A_{12}]\cdot[A_{OT1}]\cdot\left\{\overline{W}_{OT}\right\}+$$
$$+\{r_7\}^T\cdot[A_{56}]\cdot[A_{45}]\cdot[A_{34}]\cdot[A_{23}]\cdot[A_{12}]\cdot[A_{OT1}]\cdot\left\{\overline{W}_{OT}\right\};$$

$$\left\{\overline{r_H^{OT}}\right\}=\{r_1\}^T\cdot\left\{\overline{W}_{OT}\right\}+\{r_2\}^T\cdot[A_{OT1}]\cdot\left\{\overline{W}_{OT}\right\}+$$
$$+\{r_3\}^T\cdot[A_{12}]\cdot[A_{OT1}]\cdot\left\{\overline{W}_{OT}\right\}+\{r_4\}^T\cdot[A_{23}]\cdot[A_{12}]\cdot[A_{OT1}]\cdot\left\{\overline{W}_{OT}\right\}+$$
$$+\{r_5\}^T\cdot[A_{34}]\cdot[A_{23}]\cdot[A_{12}]\cdot[A_{OT1}]\cdot\left\{\overline{W}_{OT}\right\}+\{r_6\}^T\cdot[A_{45}]\cdot[A_{34}]\cdot[A_{23}]\cdot \tag{50}$$
$$\cdot[A_{12}]\cdot[A_{OT1}]\cdot\left\{\overline{W}_{OT}\right\}+\{r_7\}^T\cdot[A_{56}]\cdot[A_{45}]\cdot[A_{34}]\cdot[A_{23}]\cdot$$
$$\cdot[A_{12}]\cdot[A_{OT1}]\cdot\left\{\overline{W}_{OT}\right\}+\{r_8\}^T\cdot[A_{67}]\cdot[A_{56}]\cdot[A_{45}]\cdot[A_{34}]\cdot$$
$$\cdot[A_{23}]\cdot[A_{12}]\cdot[A_{OT1}]\cdot\left\{\overline{W}_{OT}\right\};$$

$$\left\{\overline{r_R^{OT}}\right\}=\{r_1\}^T\cdot\left\{\overline{W}_{OT}\right\}+\{r_2\}^T\cdot[A_{OT1}]\cdot\left\{\overline{W}_{OT}\right\}+$$
$$+\{r_3\}^T\cdot[A_{12}]\cdot[A_{OT1}]\cdot\left\{\overline{W}_{OT}\right\}+\{r_4\}^T\cdot[A_{23}]\cdot[A_{12}]\cdot[A_{OT1}]\cdot\left\{\overline{W}_{OT}\right\}+$$
$$+\{r_5\}^T\cdot[A_{34}]\cdot[A_{23}]\cdot[A_{12}]\cdot[A_{OT1}]\cdot\left\{\overline{W}_{OT}\right\}+\{r_6\}^T\cdot[A_{45}]\cdot[A_{34}]\cdot[A_{23}]\cdot$$
$$\cdot[A_{12}]\cdot[A_{OT1}]\cdot\left\{\overline{W}_{OT}\right\}+\{r_7\}^T\cdot[A_{56}]\cdot[A_{45}]\cdot[A_{34}]\cdot[A_{23}]\cdot[A_{12}]\cdot$$
$$\cdot[A_{OT1}]\cdot\left\{\overline{W}_{OT}\right\}+\ldots+\{r_{16}\}^T\cdot[A_{1415}]\cdot[A_{1314}]\cdot[A_{1213}]\cdot$$
$$\cdot[A_{1112}]\cdot[A_{1011}]\cdot[A_{910}]\cdot[A_{89}]\cdot[A_{78}]\cdot[A_{67}]\cdot[A_{56}]\cdot$$
$$\cdot[A_{45}]\cdot[A_{34}]\cdot[A_{23}]\cdot[A_{12}]\cdot[A_{OT1}]\cdot\left\{\overline{W}_{OT}\right\}+$$
$$+\{S_{17}\}^T\cdot[A_{1516}]\cdot[A_{1415}]\cdot[A_{1314}]\cdot[A_{1213}]\cdot[A_{1112}]\cdot$$
$$\cdot[A_{1011}]\cdot[A_{910}]\cdot[A_{89}]\cdot[A_{78}]\cdot[A_{67}]\cdot[A_{56}]\cdot[A_{45}]\cdot$$
$$\cdot[A_{34}]\cdot[A_{23}]\cdot[A_{12}]\cdot[A_{OT1}]\cdot\left\{\overline{W}_{OT}\right\} \tag{51}$$

B. Speed calculus

We follow to determine the *R* point speed depending with T_{OT} reference system. For this we differentiate successively (43) to (51), but for achieve this calculus is necessary to build the anti symmetric matrices for each joint, like the form from (52).

$$\left[\tilde{\omega}_{Cxi}\right]=\begin{bmatrix}0 & \omega_{Cxi} & -\omega_{Cxi}\\ -\omega_{Cxi} & 0 & \omega_{Cxi}\\ \omega_{Cxj} & -\omega_{Cxj} & 0\end{bmatrix},\ \text{with } i,j=\overline{1,16}. \tag{52}$$

For this:

$$\left[\dot{A}_{OT1}\right]=\left[\tilde{\omega}_{OT1}\right]\cdot[A_{OT1}];\quad \left[\dot{A}_{OT2}\right]=\left[\tilde{\omega}_{12}\right]\cdot[A_{OT2}];$$
$$\left[\dot{A}_{OT3}\right]=\left[\tilde{\omega}_{23}\right]\cdot[A_{OT3}];\quad \left[\dot{A}_{OT4}\right]=\left[\tilde{\omega}_{34}\right]\cdot[A_{OT4}];$$
$$\left[\dot{A}_{OT5}\right]=\left[\tilde{\omega}_{45}\right]\cdot[A_{OT5}];\quad \left[\dot{A}_{OT6}\right]=\left[\tilde{\omega}_{56}\right]\cdot[A_{OT6}];$$
$$\left[\dot{A}_{OT7}\right]=\left[\tilde{\omega}_{67}\right]\cdot[A_{OT7}];\quad \left[\dot{A}_{OT8}\right]=\left[\tilde{\omega}_{78}\right]\cdot[A_{OT8}];$$
$$\left[\dot{A}_{OT9}\right]=\left[\tilde{\omega}_{89}\right]\cdot[A_{OT9}];\quad \left[\dot{A}_{OT10}\right]=\left[\tilde{\omega}_{910}\right]\cdot[A_{OT10}];$$
$$\left[\dot{A}_{OT11}\right]=\left[\tilde{\omega}_{1011}\right]\cdot[A_{OT11}];\quad \left[\dot{A}_{OT12}\right]=\left[\tilde{\omega}_{1112}\right]\cdot[A_{OT12}];$$
$$\left[\dot{A}_{OT13}\right]=\left[\tilde{\omega}_{1213}\right]\cdot[A_{OT13}];\quad \left[\dot{A}_{OT14}\right]=\left[\tilde{\omega}_{1314}\right]\cdot[A_{OT13}];$$
$$\left[\dot{A}_{OT15}\right]=\left[\tilde{\omega}_{1415}\right]\cdot[A_{OT15}];\quad \left[\dot{A}_{OT16}\right]=\left[\tilde{\omega}_{1516}\right]\cdot[A_{OT16}];$$
$$\left[\dot{A}_{OT17}\right]=\left[\tilde{\omega}_{1617}\right]\cdot[A_{OT17}] \tag{53}$$

By differentiating (43) to (51) for each joint centre point we obtain the speed equations. For *A, B* and *C,* we will obtain the speed (54), (55) and (56). Similarly, we obtain the velocities of other joint centre points. The velocity for *R* point is given by (57).

$$\left\{\overline{v_A^{OT}}\right\}=0; \tag{54}$$

$$\left\{\overline{v_B^{OT}}\right\}=0+\{r_2\}^T\cdot\left[\tilde{\omega}_{OT1}\right]\cdot[A_{OT1}]\cdot\left\{\overline{W}_{OT}\right\}; \tag{55}$$

$$\left\{\overline{v_C^{OT}}\right\}=0+\{r_2\}^T\cdot\left[\tilde{\omega}_{OT1}\right]\cdot[A_{OT1}]\cdot\left\{\overline{W}_{OT}\right\}+\{r_3\}^T\cdot \tag{56}$$
$$\cdot\left[\tilde{\omega}_{12}\right]\cdot[A_{OT2}]\cdot\left\{\overline{W}_{OT}\right\};$$

$$\left\{\overline{v_R^{OT}}\right\}=0+\{r_2\}^T\cdot\left[\tilde{\omega}_{OT1}\right]\cdot[A_{OT1}]\cdot\left\{\overline{W}_{OT}\right\}+\{r_3\}^T\cdot\left[\tilde{\omega}_{12}\right]\cdot$$
$$\cdot[A_{OT2}]\cdot\left\{\overline{W}_{OT}\right\}+\{r_4\}^T\cdot\left[\tilde{\omega}_{23}\right]\cdot[A_{OT3}]\cdot\left\{\overline{W}_{OT}\right\}+\{r_5\}^T\cdot \tag{57}$$
$$\cdot\left[\tilde{\omega}_{34}\right]\cdot[A_{OT4}]\cdot\left\{\overline{W}_{OT}\right\}+\{r_6\}^T\cdot\left[\tilde{\omega}_{45}\right]\cdot[A_{OT5}]\cdot\left\{\overline{W}_{OT}\right\}+$$
$$+\ldots+\{r_{15}\}^T\cdot\left[\tilde{\omega}_{1314}\right]\cdot[A_{OT14}]\cdot\left\{\overline{W}_{OT}\right\}+\{r_{16}\}^T\cdot\left[\tilde{\omega}_{1415}\right]\cdot$$
$$\cdot[A_{OT15}]\cdot\left\{\overline{W}_{OT}\right\}+\{S_{17}\}^T\cdot\left[\tilde{\omega}_{1516}\right]\cdot[A_{OT16}]\cdot\left\{\overline{W}_{OT}\right\}$$

C. Acceleration calculus

These will be obtained by differentiating successively the speed equations. For *A,* and *B,* we will obtain the accelerations (58) and (59). Similarly, we obtain the accelerations of other joint centre points. The acceleration for *R* point is given by (60).

$$\left\{\overline{a}_A^{OT}\right\} = 0; \tag{58}$$

$$\left\{\overline{a}_B^{OT}\right\} = 0 + \{r_2\}^T \cdot \left[\dot{\tilde{\omega}}_{OT1}\right] \cdot [A_{OT1}] \cdot \{\overline{W}_{OT}\} + \{r_2\}^T \cdot \left[\tilde{\omega}_{OT1}\right] \cdot \left[\tilde{\omega}_{OT1}\right] \cdot [A_{OT1}] \cdot \{\overline{W}_{OT}\} \tag{59}$$

$$\begin{aligned}\left\{\overline{a}_R^{OT}\right\} = 0 &+ \{r_2\}^T \cdot \left[\dot{\tilde{\omega}}_{OT1}\right] \cdot [A_{OT1}] \cdot \{\overline{W}_{OT}\} + \{r_2\}^T \cdot \left[\tilde{\omega}_{OT1}\right] \cdot \left[\tilde{\omega}_{OT1}\right] \cdot [A_{OT1}] \cdot \{\overline{W}_{OT}\} + \{r_3\}^T \cdot \left[\dot{\tilde{\omega}}_{12}\right] \cdot [A_{OT2}] \cdot \{\overline{W}_{OT}\} + \{r_3\}^T \cdot \left[\tilde{\omega}_{12}\right] \cdot \left[\tilde{\omega}_{12}\right] \cdot [A_{OT2}] \cdot \{\overline{W}_{OT}\} + \{r_4\}^T \cdot \left[\dot{\tilde{\omega}}_{23}\right] \cdot [A_{OT3}] \cdot \{\overline{W}_{OT}\} + \{r_4\}^T \cdot \left[\tilde{\omega}_{23}\right] \cdot \left[\tilde{\omega}_{23}\right] \cdot [A_{OT3}] \cdot \{\overline{W}_{OT}\} + \{r_5\}^T \cdot \left[\dot{\tilde{\omega}}_{34}\right] \cdot [A_{OT4}] \cdot \{\overline{W}_{OT}\} + \ldots + \{r_{15}\}^T \cdot \left[\dot{\tilde{\omega}}_{1314}\right] \cdot [A_{OT14}] \cdot \{\overline{W}_{OT}\} + \{r_{15}\}^T \cdot \left[\tilde{\omega}_{1314}\right] \cdot \left[\tilde{\omega}_{1314}\right] \cdot [A_{OT14}] \cdot \{\overline{W}_{OT}\} + \{r_{16}\}^T \cdot \left[\dot{\tilde{\omega}}_{1415}\right] \cdot [A_{OT15}] \cdot \{\overline{W}_{OT}\} + \{r_{16}\}^T \cdot \left[\tilde{\omega}_{1415}\right] \cdot \left[\tilde{\omega}_{1415}\right] \cdot [A_{OT15}] \cdot \{\overline{W}_{OT}\} + \\ + \{S_{17}\}^T \cdot \left[\dot{\tilde{\omega}}_{1516}\right] \cdot [A_{OT16}] \cdot \{\overline{W}_{OT}\} + \{S_{17}\}^T \cdot \left[\tilde{\omega}_{1516}\right] \cdot \left[\tilde{\omega}_{1516}\right] \cdot [A_{OT16}] \cdot \{\overline{W}_{OT}\}\end{aligned} \tag{60}$$

D. Numerical processing

For cinematic analysis, the geometrical elements are known. The computing algorithm was elaborated with the MAPLE aid. The geometrical elements dimensions are in millimeters: L_{OT}=70; L_1=65; L_2=65; L_3=200; L_4=5; L_5=225; L_6=5; L_7=5; L_8=220; L_9=5; L_{10}=5; L_{11}=225; L_{12}=5; L_{13}=200; L_{14}=65; L_{15}=65; L_{16}=70. The generalized coordinate system variations for the equivalent locomotion system active joints in walking activity's case are presented in Fig. 11, Fig. 12, Fig. 13, Fig. 14, Fig. 15 and Fig.16. These were processed in a 4 and 7 years old children. The angular amplitudes of these motion laws were validated by consulting specialty literature data and represents a single gait for walking [8], [9], [10], [27].

The 4 years old children segment represents the lower limit for the desired design parameters and the 7 years old children segment represents the upper limit.

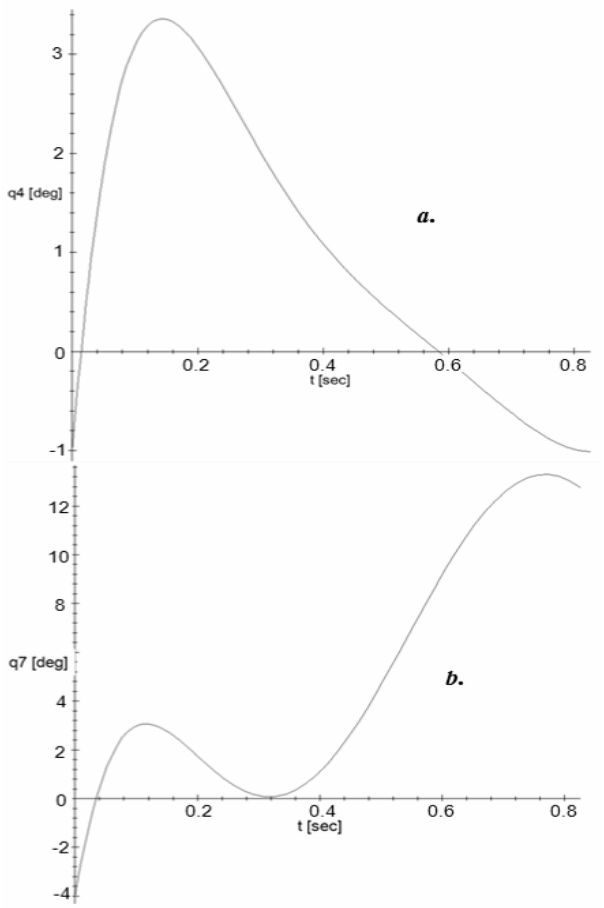

Fig. 11. Generalized coordinate motion law equivalent with the hip joint for walking activity in the case of a 4 year old child: a-left lower limb; b-right lower limb.

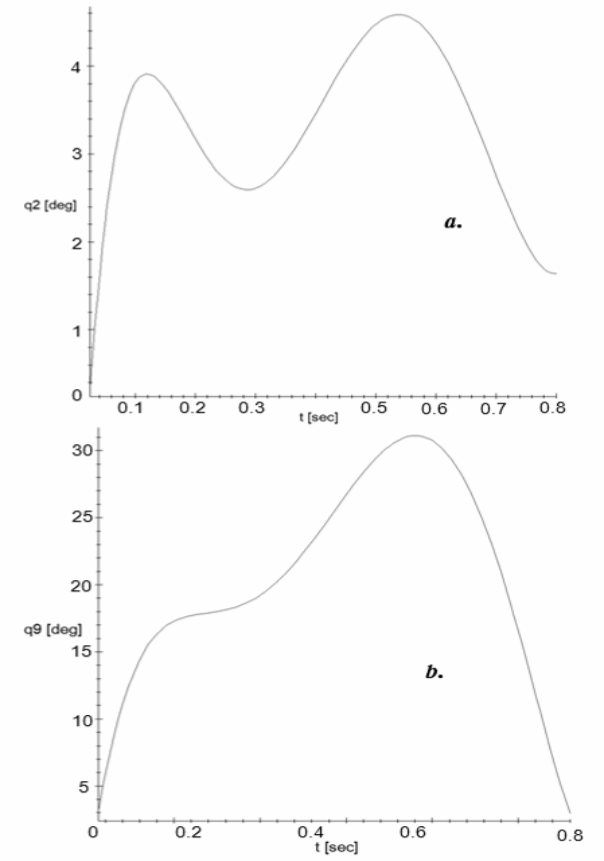

Fig. 12. Generalized coordinate motion law equivalent with the knee joint for walking activity in the case of a 4 year old child: a-left lower limb; b-right lower limb.

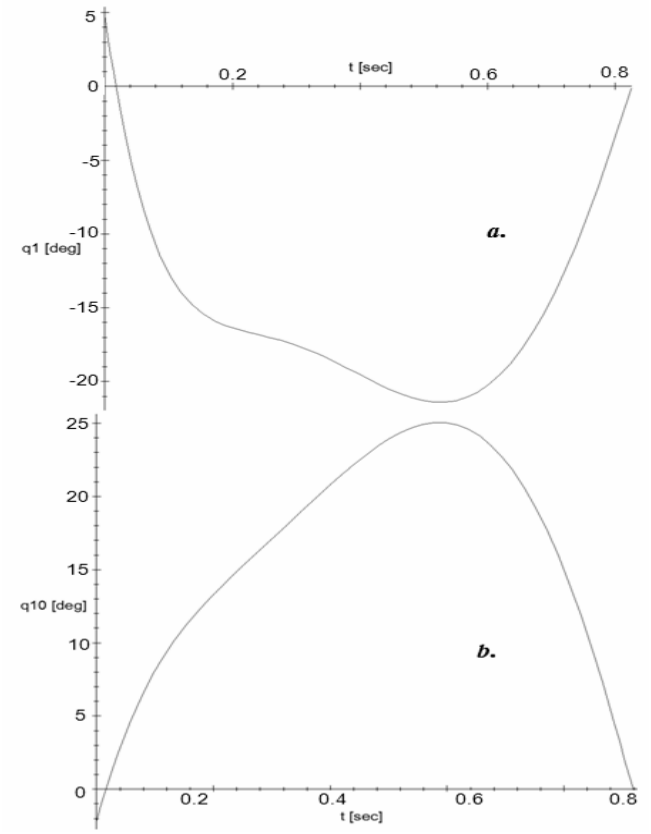

Fig. 13. Generalized coordinate motion law equivalent with the ankle joint for walking activity in the case of a 4 year old child: a-left lower limb; b-right lower limb.

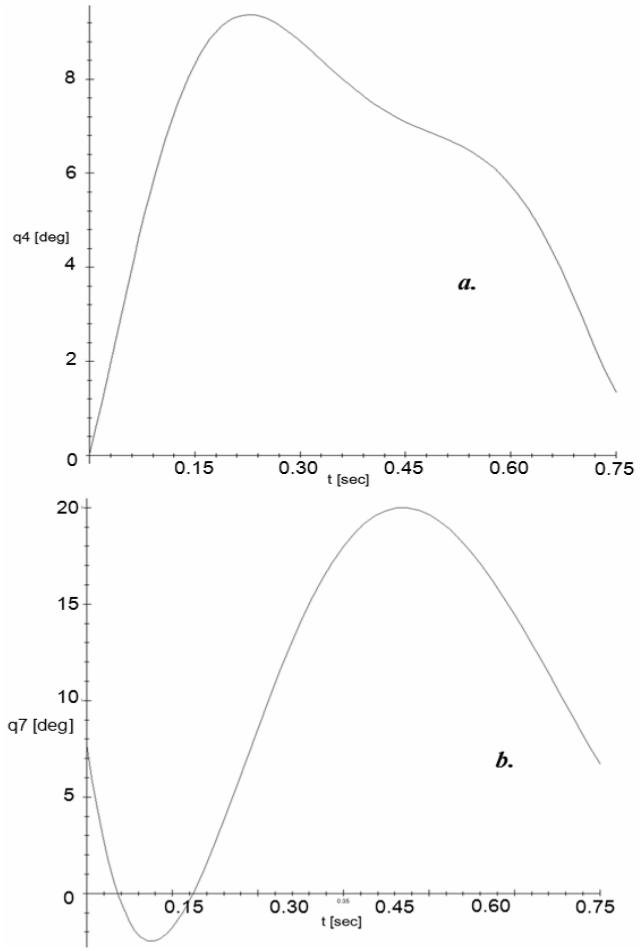

Fig. 14. Generalized coordinate motion law equivalent with the hip joint for walking activity in the case of a 7 year old child: a-left lower limb; b-right lower limb.

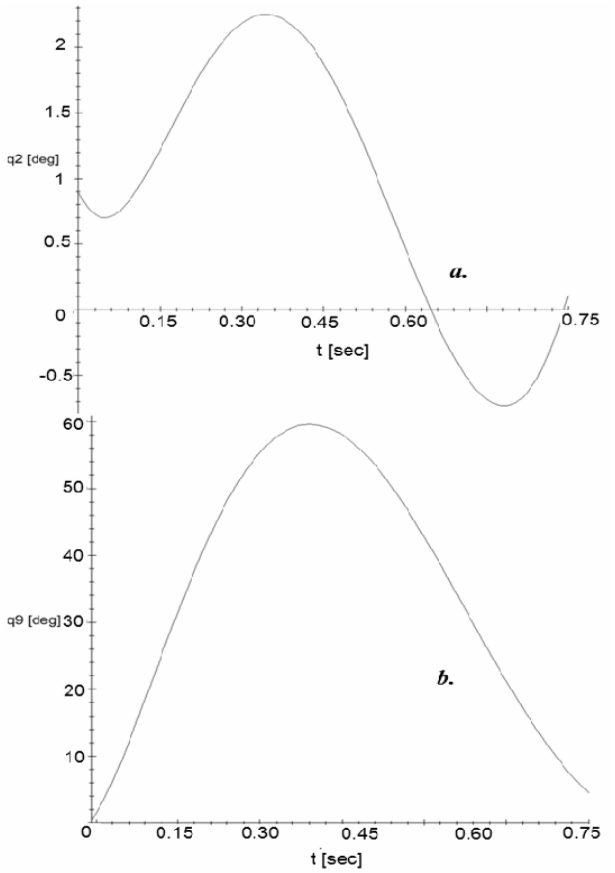

Fig. 15. Generalized coordinate motion law equivalent with the knee joint for walking activity in the case of a 7 year old child: a-left lower limb; b-right lower limb.

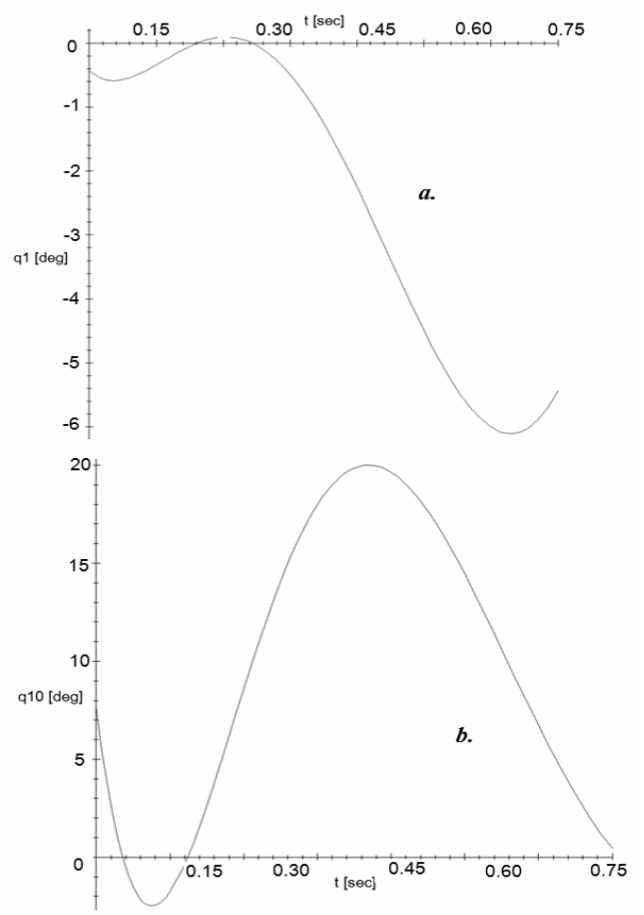

Fig. 16. Generalized coordinate motion law equivalent with the ankle joint for walking activity in the case of a 7 year old child: a-left lower limb; b-right lower limb.

IV. Children locomotion system dynamic analysis

The dynamic analysis aim is to identify the connection forces variation laws depending on time. Mathematical models adopted were designed so that we can develop an interface with finite element method. This interface will allow excitation of each joint in normal operating conditions or critical ones appropriate with those existent in reality. The correct finality of this objective is guaranteed by the design of the integrated dynamic model - experiment, finite element modeling and simulations.

A mathematical model used for inverse dynamic analysis of the human lower limb, will be elaborated by taking in account the ground contact. This dynamic model starts from the cinematic scheme presented in Fig. 10. Similar analysis and procedures can be found in [1], [4], [6], [7], [12], [14], [16] and [26]. Input data: For an inverse dynamic analysis one consider known the geometric elements (L_{OT}, L_1, L_2… L16) and generalized coordinates variation laws from cinematic joints: q_1, q_2, q_3,…,q_{16} obtained from cinematic analysis. A calculus algorithm was elaborated with MAPLE software's aid. Output data: It will be followed to obtain the connection forces components, which will appear in the walking activity, for a gait cycle, at the each joint level from the mathematical model structure which is equivalent to human locomotion system. The constraint equations are:

$$\Phi(q, t) = 0. \tag{61}$$

q_r - Generalized coordinates vector considered when the elements are rigid ones; t- time.

Or customizing for „i" elements, we obtain:

$$\overrightarrow{q_i} = \left[\left\{ r_{Ci}^{Tcx} \right\}^T, \varphi_i \right]^T; \tag{62}$$

$$\left[r_{Ci}^{Tcx} \right]^T = \left\{ X_{Ci}^{Tcx}, Y_{Ci}^{Tcx}, Z_{Ci}^{Tcx} \right\}; \tag{63}$$

Will make the following notations:

$$X_i = X_{Ci}^{Tcx}; Y_i = Y_{Ci}^{Tcx}; Z_i = Z_{Ci}^{Tcx}; \tag{64}$$

$$\begin{cases} X_i - X_{Ci}^{Tcx} = 0 \\ Y_i - Y_{Ci}^{Tcx} = 0 \\ Y_i - Y_{Ci}^{Tcx} = 0 \end{cases} \tag{65}$$

From where shall obtain:

$$\begin{cases} x_{Ci}^{Tcx} - Ex_i = 0 \\ y_{Ci}^{Tcx} - Ey_i = 0 \\ z_{Ci}^{Tcx} - Ez_i = 0 \end{cases}, \text{ with: } i = \overline{1,16}. \tag{66}$$

By differentiating relation (61) depending on time, will be obtained:

$$J_q \dot{q} + \frac{\partial \phi}{\partial t} = 0 \tag{67}$$

Or relations (66):

$$\begin{cases} \dot{x}_{Ci}^{Tcx} - \frac{\partial}{\partial t} X_{Ci}^{Tcx} = 0 \\ \dot{y}_{Ci}^{Tcx} - \frac{\partial}{\partial t} Y_{Ci}^{Tcx} = 0 . \\ \dot{z}_{Ci}^{Tcx} - \frac{\partial}{\partial t} Z_{Ci}^{Tcx} = 0 \end{cases} \tag{68}$$

We differentiate relation (67) depending on time, and we obtain:

$$J_q \cdot \ddot{q} + \left(J_q \cdot \dot{q} \right)_q \cdot \dot{q} + \frac{\partial^2 \phi}{\partial t^2} + 2 \dot{J}_q \cdot \dot{q} = 0 \tag{69}$$

By differentiating relations no (68) in rapport with time, we obtain:

$$\begin{cases} \ddot{x}_{Ci}^{Tcx} - \frac{\partial^2}{\partial t^2} Ex_i = 0 \\ \ddot{y}_{Ci}^{Tcx} - \frac{\partial^2}{\partial t^2} Ey_i = 0 \\ \ddot{z}_{Ci}^{Tcx} - \frac{\partial^2}{\partial t^2} Ez_i = 0 \end{cases} \tag{70}$$

Equations no (67) and (69) can be written in a compact form by introducing the notations:

$$J_q \cdot \dot{q} = -\frac{\partial \Phi}{\partial t} = v \tag{71}$$

$$J_q \cdot \ddot{q} = -2 \dot{J}_q \cdot \dot{q} - \left(J_q \cdot \dot{q} \right)_q \cdot \dot{q} - \frac{\partial^2 \phi}{\partial t^2} = a \tag{72}$$

The mechanical work of mass forces is:

$$\delta L = \delta r_{C1}^{Tcx} \cdot G_1 + \delta r_{C2}^{Tcx} \cdot G_2 + \ldots + \delta r_{C16}^{Tcx} \cdot G_{16} = \sum_{i=1}^{16} \delta r_{Ci}^{Tcx} \cdot G_i \tag{73}$$

The motion equation has the following form:

$$\begin{bmatrix} M & J_q^T \\ J_q & 0 \end{bmatrix} \begin{bmatrix} \ddot{q} \\ \lambda \end{bmatrix} = \begin{bmatrix} Q_a \\ a \end{bmatrix}. \tag{74}$$

Where: M, represents the mass matrix with:

$$M = diag\,(m_i, J_i);\ i = \overline{1,16}\,. \tag{75}$$

The vector of active forces:

$$Q_a = \begin{bmatrix} 0\ 0\ -m_1 q\ 0,\ 0\ 0\ 0\ -m_2 q,\ldots, \\ 0\ 0\ -m_{15} q\ 0,\ 0\ 0\ 0\ -m_{16} q \end{bmatrix}^T \tag{76}$$

A mathematical relation between mass matrix and the active forces vector is given by:

$$M \cdot \ddot{q} + J_q \cdot \lambda = Q_a \tag{77}$$

We obtain the Lagrange's multipliers are:

$$\lambda = \left[J_q\right]^{-1}\left[Q_a - M \cdot \ddot{q}\right]. \tag{78}$$

The motion laws are known: $q(t)$, $\dot{q}(t)$ and $\ddot{q}(t)$, from the cinematic analysis. From (78) we determine λ Lagrange's multipliers, with the aid of a programming algorithm accomplished in MAPLE software. With these it will be process an inverse dynamic analysis from it were obtained joint connection forces. These forces were determined by taking into account the Lagrange multipliers:

$$F_i^{"r(i,j)} = [R_{i,i"}]^T \cdot [A_{oi}]^T \cdot [\lambda]^{r(i,j)} \tag{79}$$

Based on the elaborated algorithm the connection forces for each joint were obtained. The joints are from the model presented above, and the connection forces components are oriented on 3 directions for a xyz coordinate system.

The force components for knee joint are presented in Fig. 17 and Fig. 18, and are used to design orthotic and prosthetic mechanisms especially for children on 4-7 years age. The high values and high oscillations onto these diagrams are from the foot with ground contact when the analyzed subjects are in the Tst and Tsw gait phases.

The knee connection force value in case of a 4 year old child is 9.845N on swing phase. In case of a 7 year old child, the knee connection force is 18.908N on swing phase. This data help us to design orthotics and prosthesis mechanisms. In order to validate these mechanisms is necessary to simulate with Dynamic Module from MSC Adams environment.

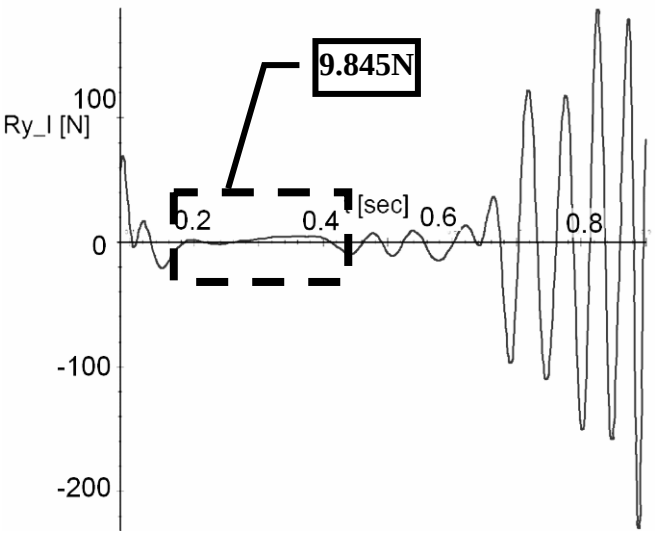

Fig. 17. Connection force component on Y direction for knee articulation (I-joint) [Newton] vs. time [sec] for 4 years children segment

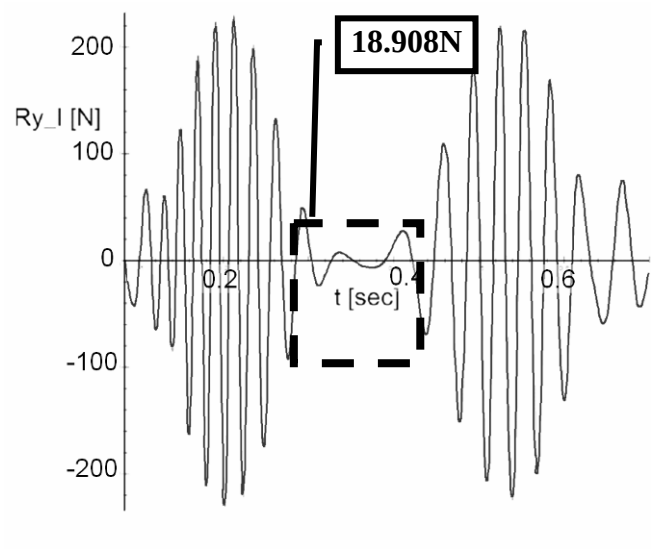

Fig. 18. Connection force component on Y direction for knee articulation (I-joint) [Newton] vs. time [sec] for 7 years children segment

V. Orthotics and Prosthesis Design Based on Dynamic Considerations

Based on the dynamic analysis presented here, the obtained results are useful for design a knee modular orthosis for 4-7 years old children and a parameterized knee prosthesis which has a cam mechanism in his structure. The virtual models are presented in Fig. 19 and Fig. 23.

For virtual simulations the knee modular orthosis was imported in MSC Adams Environment by creating an export interface from SolidWorks. Two virtual models were created, one for a 4 years old child and other for 7 years old as it shown in Fig 19 - a, b.

As a dynamic viewpoint for knee modular orthotics through virtual simulations it wants to be determinate the cable forces for both cases. For this the connection forces components from Fig. 17 and Fig. 18 were applied on knee orthotics final module.

The connection force from figure 17 was applied in case of the modular knee orthosis from Fig. 19-a, and the other connection force from Fig. 18 for the virtual model from Fig. 19-b.

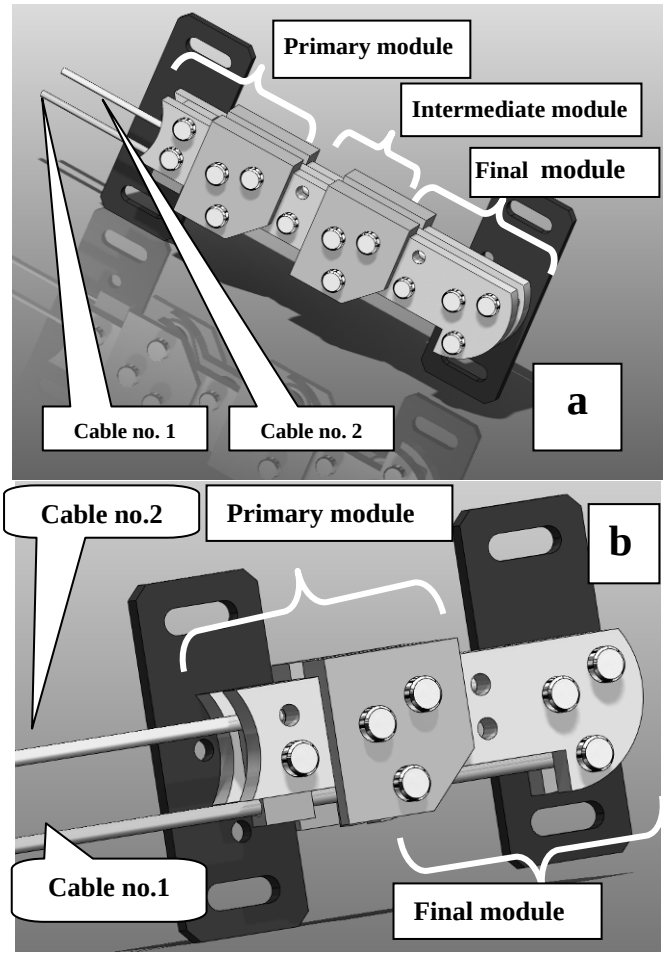

Fig. 19. Knee modular orthosis virtual model with components identification (a-case of a 7 years old child; b-case of a 4 years old child).

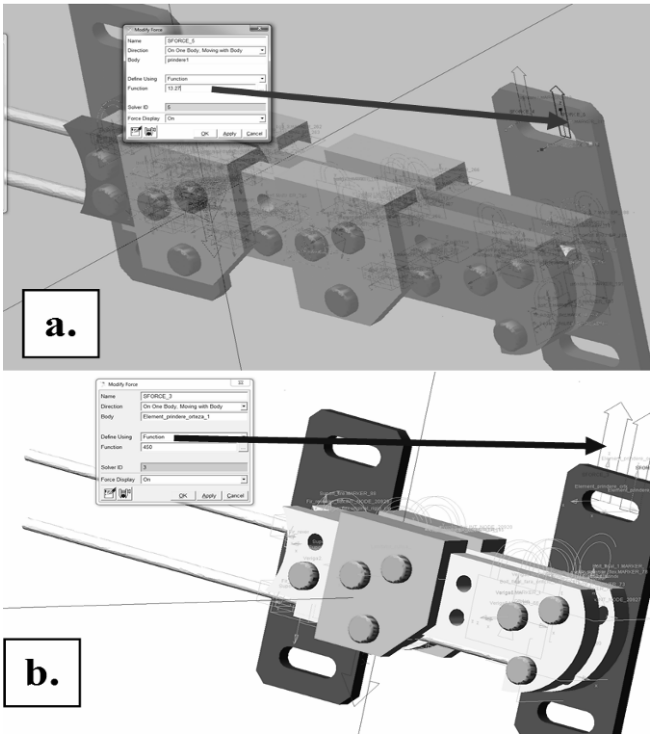

Fig. 20. Aspects regarding the applied force laws (a-case of a 7 years old child; b-case of a 4 years old child).

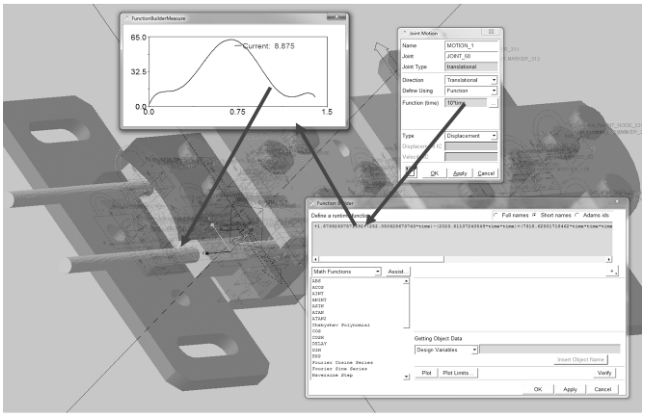

Fig. 21. Defining the modular orthosis motion in case of a 7 years old child.

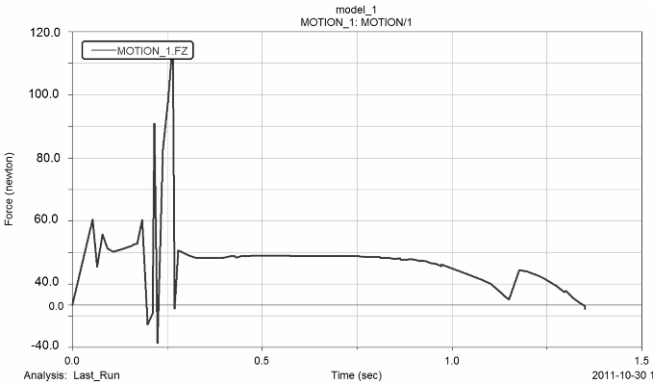

Fig. 22. Force variation diagram for cable no. 1 of the knee modular orthosis in a 7 years old child case.

In Fig. 20 and Fig. 21, an aspect of virtual models in the MSC Adams environment is shown (applying the force laws and knee motion definition).

The forces from cables are presented in Fig. 22 and Fig. 23. It can be observe that the maximum value is 112.5N for a 7 years old child, which means that the cable diameters are correctly choose.

The diameter in this case is a 1.75 millimeters stainless steel. In the 4 years old child case this was smaller and the obtained value was 68.75N (Fig. 23).

In the knee parameterized prosthesis case, presented in Fig. 24, the component identification is: 1-femur component, 2-cilindrical joint, 3- cam follower, 4- cam, 5-tibia component, 6-FESTO shock absorber, 7-aditional shock absorber mechanism. For this through VisualNastran simulations dynamic response was determined.

Dynamic response was represented through von Misses stress, displacements and deformations of the knee prosthesis mechanism.

These results were obtained in a dynamic mode by applying the connection forces from figure 18 onto femur element, and the knee motion law from figure 15 was applied onto the drive element for a single gait.

The drive element was the Festo shock absorber. The foot element was considered as fixed one and at knee joint level, as it shown in Fig. 25

The results are shown in Fig. 26, Fig. 27 and Fig. 28. Von Misses stress average value was 21 MPa, displacements were 0.034milimeters and total deformations were 0.000061. Also the variation diagrams of these results are shown in Fig. 29, Fig. 30 and Fig. 31.

These values were obtained for aluminum alloys which confer a small weight and can be easy to wear for the children with one amputated leg.

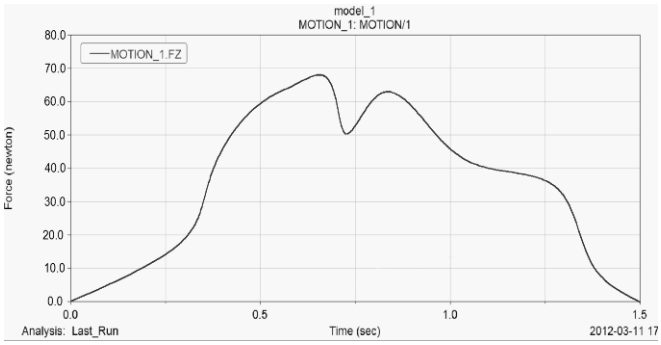

Fig. 23. Force variation diagram for cable no. 1 of the knee modular orthosis in a 4 years old child case.

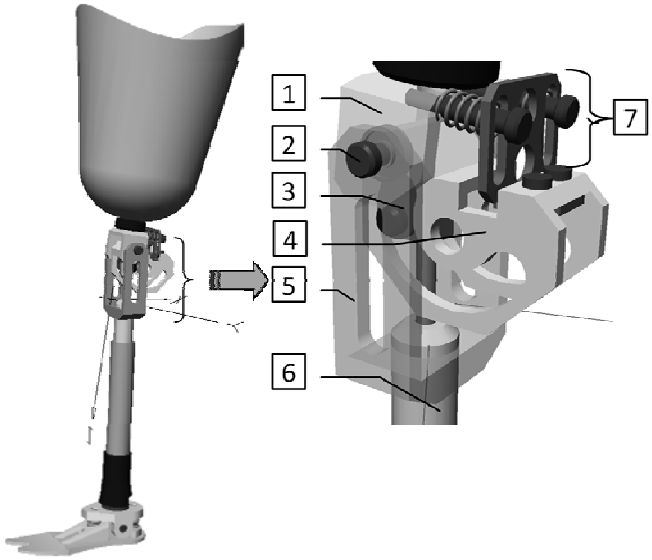

Fig. 24. Parameterized knee prosthesis for 4-7 years old children with component identification

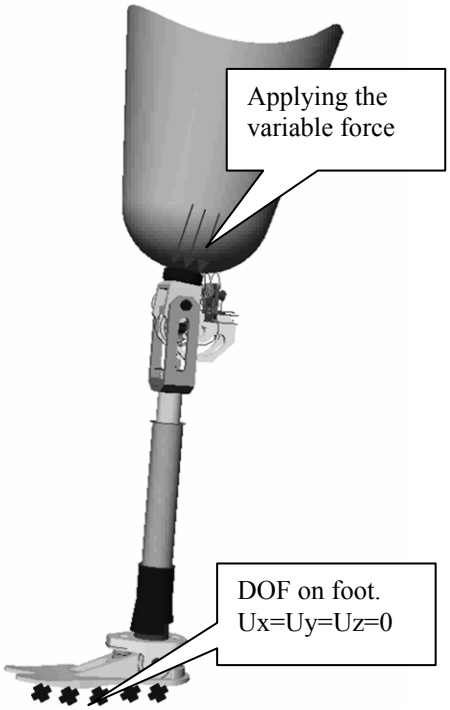

Fig. 25. Applying loads and establishing the DOF conditions for the parameterized knee prosthesis for 4-7 years old children

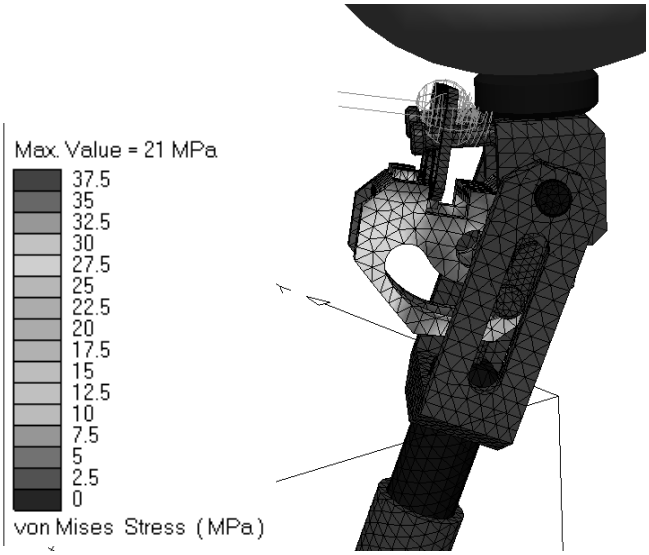

Fig. 26. Von Misses stress of the parameterized knee prosthesis

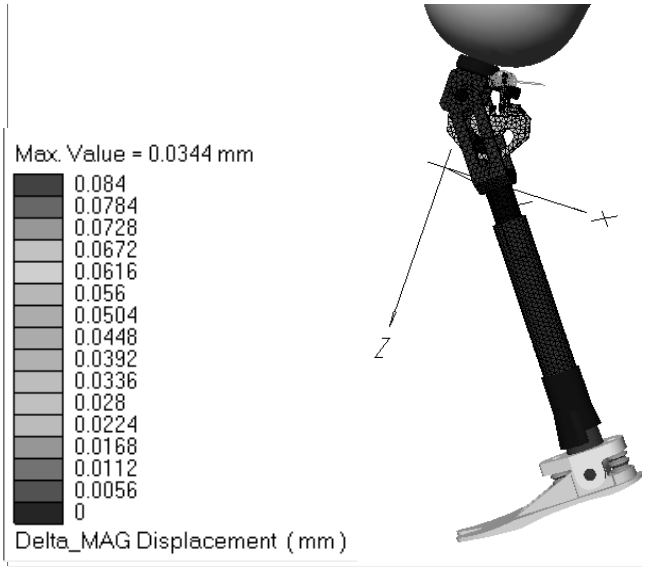

Fig. 27. Displacements of the parameterized knee prosthesis

Fig. 28. Deformations of the parameterized knee prosthesis

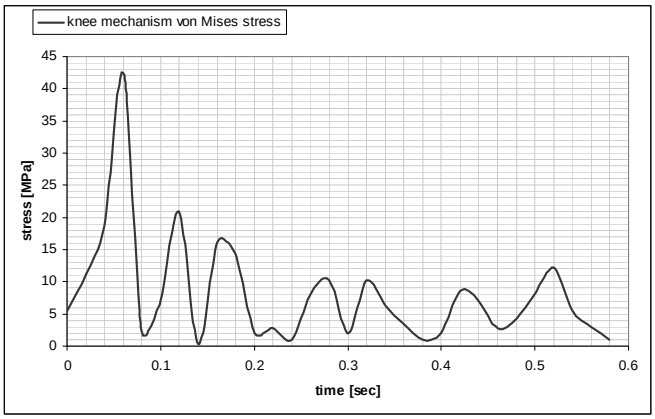

Fig. 29. Von Misses stress of the parameterized knee prosthesis variation during one gait depending on time

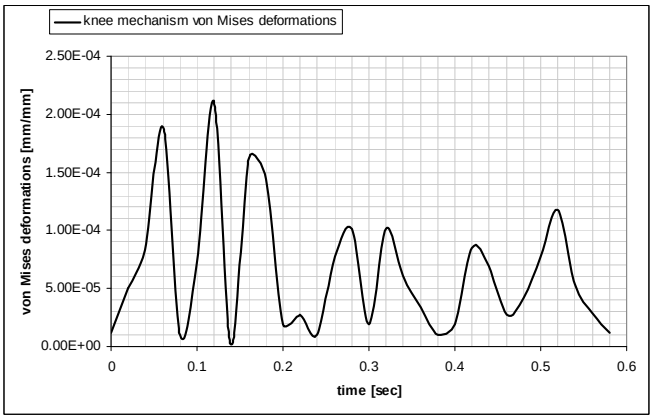

Fig. 30. Deformations of the parameterized knee prosthesis variation during one gait depending on time

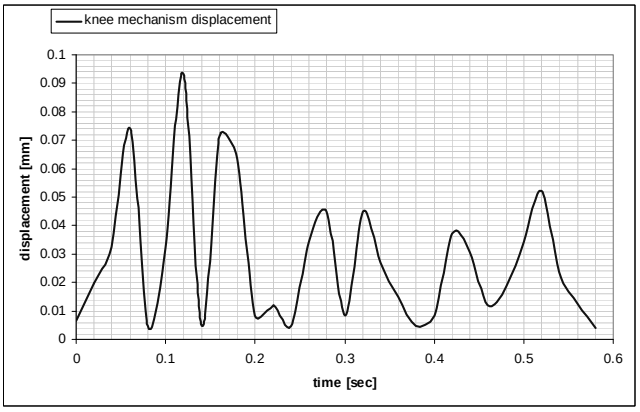

Fig. 31. Displacements of the parameterized knee prosthesis variation during one gait depending on time

VI. Conclusion

As final conclusions it can be mentioned that this type of analysis has an original approach because it was started by creating a database from an experimental research and finally to obtain connection forces diagrams used for orthotics and prosthesis design. With these it can be presented here real models of a modular knee orthotic device (Fig. 32, Fig. 33, Fig. 34, Fig. 35 and Fig. 36) and parameterized knee prosthesis (Fig. 39 and Fig. 40).

The motion laws developed through the experimental research can be useful to joint actuators program and control from an exoskeleton structure specially designed for children with temporal locomotion disabilities according with biomechanical features of children.

Fig. 32. Prototype experimental research in case of a 4 years old child

The experimental tests of both knee modular orthosis are validated by testing these on children with locomotion disabilities. These prototypes were tested on two children, one of a 4 years old and other of a 7 years old. The acquisition data used in this case was the CONTEMPLAS Motion Analysis equipment. The results are presented in diagrams from Fig. 37 and Fig. 38.

In these diagrams one it can be observed that the motion variation law is almost the same as in case of a healthy child.

The angular amplitudes and lower limb segments dimensions are used as entry data for dynamic analysis. Also the angular amplitudes represent the motion laws which dictate the prosthetic and orthotic devices motions specially designed for children.

Fig. 33. Prototype experimental research in case of a 7 years old child

If we analyzed the joints values movement during the gait cycle we can observe difference between group of age and this is important for design the assistive devices in according with biomechanical features of children.

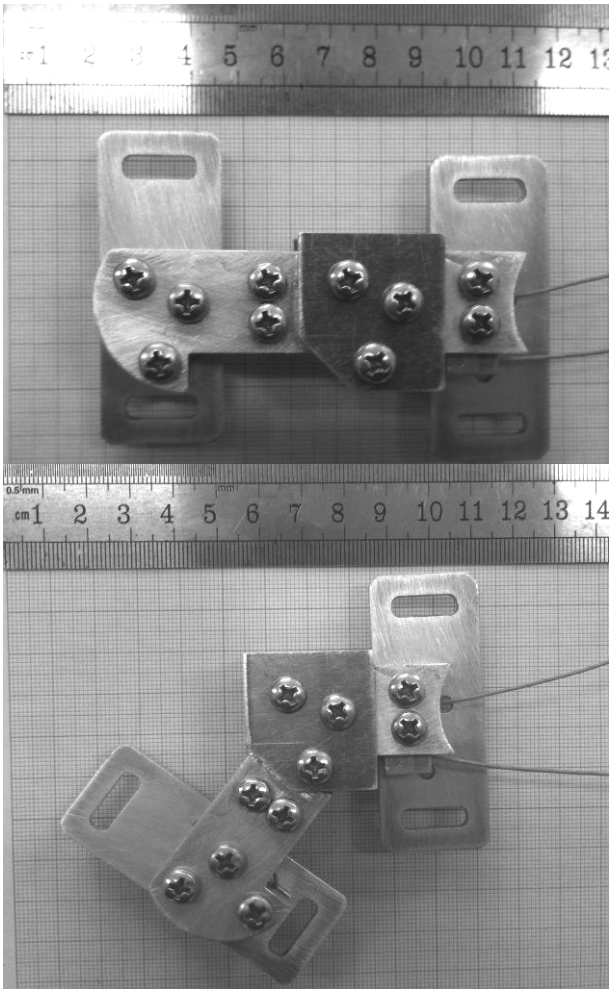

Fig. 34. Prototype experimental research in case of a 4 years old child

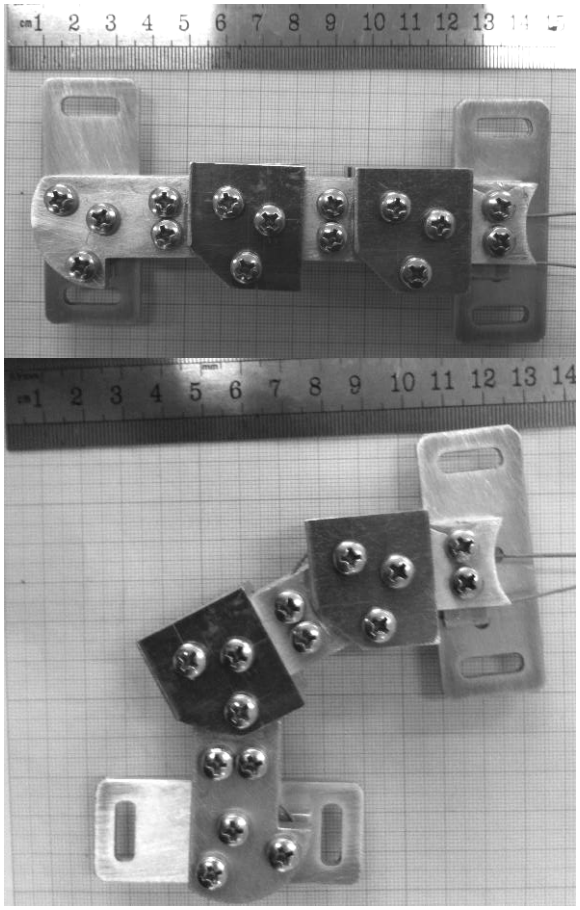

Fig. 35. Prototype experimental research in case of a 7 years old child

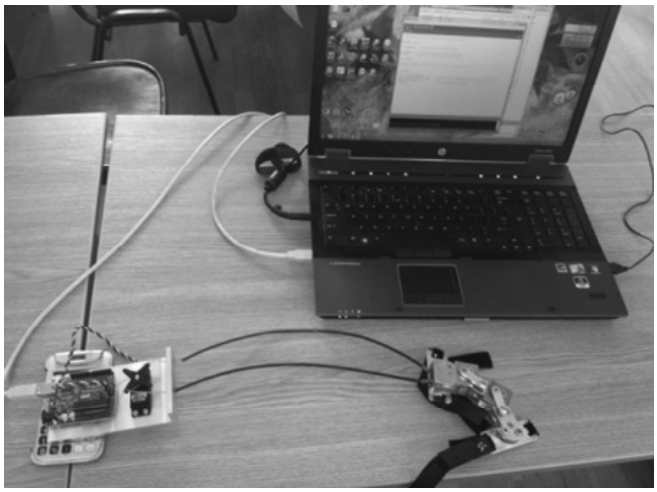

Fig. 36. Aspect regarding the knee modular orthosis command and control motion

The database that we try to create beginning from healthy people, in this research, help us to design the assistive devices for children with neuromotor pathology, depending of age and anthropometric features that means an improvement and development of fast and well rehabilitation program.

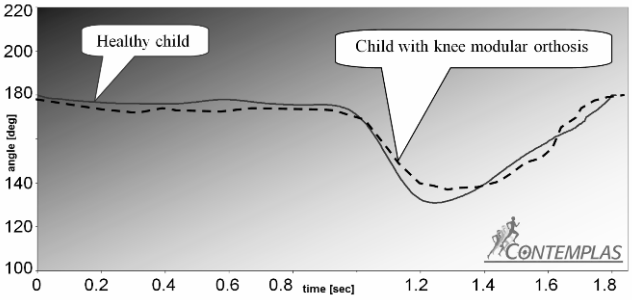

Fig. 37. Angular amplitude in case of a 4 years old child

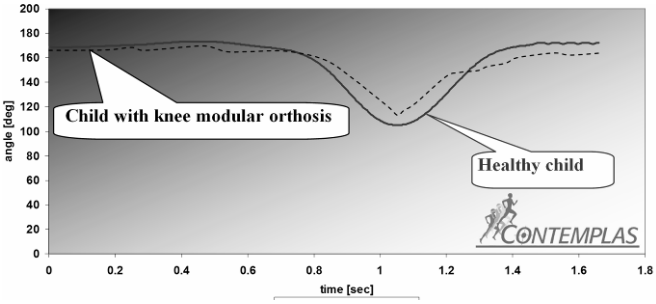

Fig. 38. Angular amplitude in case of a 7 years old child

Analyzed of joints kinematics for each phase of gait help us for design the construction of assistive devices and improvement the motor control for each joint in according with biomechanical rules. That means to improve the movement and stability of joint without decrease the role of dynamic stability involved by muscle system. Much more is possible to integrate the movement pattern of child in normal pattern of gait and to improve the balance during gait.

Analyzing the forces from Fig. 8 and Fig. 9, it help us to training the muscle group close to normal pattern of gait, because the assistive devices can involve a normal pattern of gait. So is possible to restore or to improve the normal central nervous system activity in the situations o cerebral palsy. The system of assessment the gait phase using

biomechanical assessment can help to monitoring the rehabilitation program and to develop the skills for each phase of gait, at each joint.

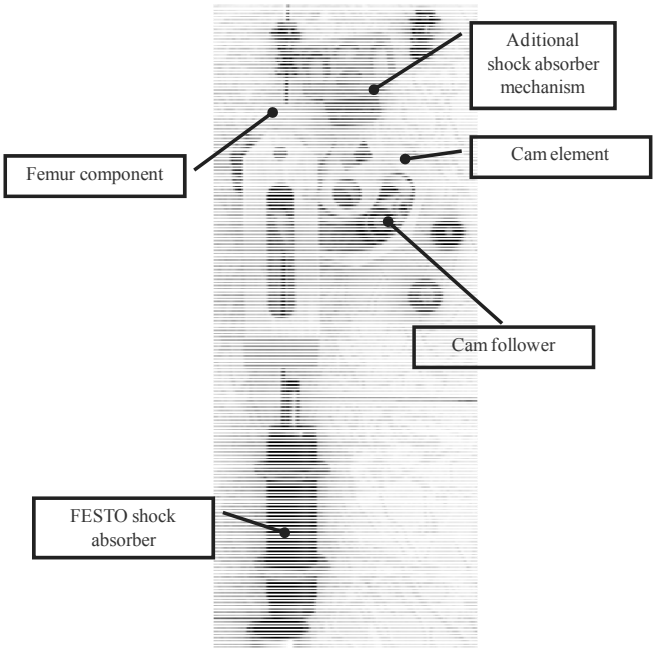

Fig. 39. Real model of parameterized knee prosthesis for children (exploded view)

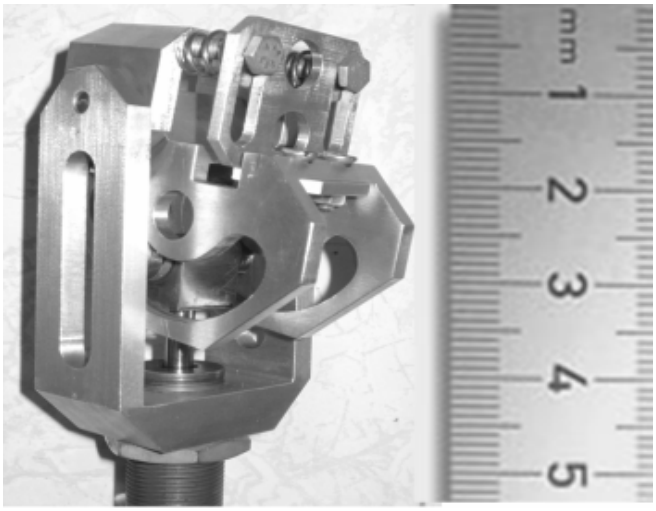

Fig. 40. Real model of parameterized knee prosthesis for children

The knee angular amplitude obtained on experimental tests by a 7-years old child with an amputated leg is 63degrees for one gait (Fig. 41).

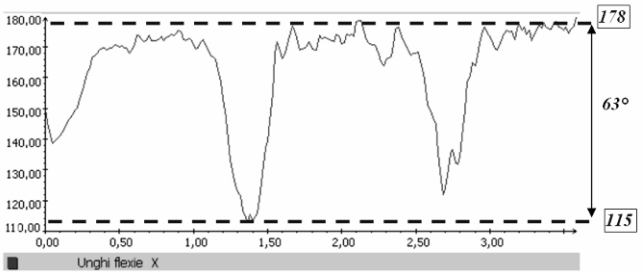

Fig. 41. The new knee prosthesis flexion/extension angular displacement variation, depending on time.

According with the experimental tests and the literature data [25], [27], this value certificate the parameterized knee prosthesis prototype.

The major problem for knee prosthesis mechanical system is the fabrication procedures, which are expensive. In the knee orthosis case the problems consists in its size, which is bigger than some children knee articulation size. On the future the research presented here will be continued in order to increase the mechanical systems performances.

ACKNOWLEDGMENT

This work was supported by the strategic grant POSDRU/89/1.5/S/61968, Project ID61968 (2009), co-financed by the European Social Fund within the Sectorial Operational Program Human Resources Development 2007-2013.

REFERENCES

[1] F. Amirouche, Computational methods in multibody dynamics. Prentice-Hall Publishing House. 1992.

[2] R. M. Kiss, L. Kocsis, and Z. Knoll, Joint kinematics and spatial temporal parameters of gait measured by an ultrasound-based system. J. Med. Eng. Phys., vol. 26:611–620. 2004.

[3] G. A. Sohl, and J. E. Bobrow, A Recursive Multibody Dynamics and Sensitivity Algorithm for Branched Kinematic Chains. ASME J. Dyn. Syst., Meas., Control, 123_3: 391–399. 2001.

[4] F. C. Anderson, and M. G. Pandy, Dynamic Optimization of Human Walking. J. Biomech. Eng., 123_5: 381–390. 2001.

[5] C., Copilusi, N., Dumitru, A., Margine. "Modular Knee Orthosis FEM Analysis from Kinematic Considerations". New Trends in Mechanism and Machine Science Mechanisms and Machine Science. Vol. 7, 2012, pp 431-439.

[6] C., Copilusi, M., Marin, L., Rusu, I., Geonea, "Design Considerations regarding a New Knee Orthosis" *Journal of Applied Mechanics and Materials* Vol. 162. 2012. Online available since 2012/Mar/27 at www.scientific.net. pp 276-285.

[7] C. Copilusi, M. Marin, N. Dumitru, L. Rusu , "Locomotion System Dynamic Analysis with Application on Children Orthotics and Prostheses Devices". *Lecture Notes in Engineering and Computer Science: World Congress on Engineering.* Vol. III. 2012. pp. 1663-1668.

[8] C. Copilusi, " Design of a New Knee Modular Orthotic Device from Cinematic Considerations". *Lecture Notes in Engineering and Computer Science: World Congress on Engineering.* Vol. III. 2012. pp. 2010-2015.

[9] C., Copilusi, N., Dumitru, M., Marin, L., Rusu „Human Lower Limb Kinematic Analysis with Application on Prosthesis Mechanical Systems". 13th World Congress in Mechanism and Machine Science, Guanajuato, México. IMD-123. IfTOMM-2011. Paper ID: A22-343. ISBN 978-607-441-131-7.

[10] C. Copilusi, M., Marin, L., Rusu, "A New Knee Prosthesis Design Based on Human Lower Limb Cinematic Analysis" in *Lecture Notes in Engineering and Computer Science: World Congress on Engineering* Vol. III. 2011. pp. 2491–2496.

[11] C., Copiluşi, N., Dumitru, L., Rusu, M., Marin „Cam Mechanism Kinematic Analysis used in a Human Ankle Prosthesis Structure". *Lecture Notes in Engineering and Computer Science: World Congress on Engineering*. Vol. II. 2010. pp. 1316-1320.

[12] C., Copilusi, "Researches regarding some mechanical systems applicable in medicine". *PhD. Thesis, Faculty of Mechanics, University of Craiova. Romania.* 2009.

[13] CONTEMPLAS Motion Equipment. User Manual. Available: http://www.contemplas.com.

[14] N., Dumitru, C., Copilusi, M., Marin, L., Rusu. „Human Lower Limb Dynamic Analysis with Applications to Orthopedic Implants". Mechanisms and Machine Science– New Trends in Mechanism Science. Analysis and Design. Springer Berlin Heidelberg Publishing house. Vol. V. 2010. pp. 327-334.

[15] N.,Dumitru C., Copiluşi A., Zuhair. "Dynamic Modeling of a Mobile Mechanical System with Deformable Elements". *Lecture Notes in Engineering and Computer Science: World Congress on Engineering*. 2009. Vol. II. pp. 1315-1320

[16] N. Dumitru, G. Nanu, D. Vintilă, Mechanisms and mechanical transmissions. Modern and classical design techniques. Didactic printing house, ISBN 978-973-31-2332-3, Bucharest. 2008.
[17] N., Dumitru, M., Cherciu, Z., Althalabi, "Theoretical and Experimental Modelling of the Dynamic Response of the Mechanisms with Deformable Kinematics Elements". *Proceedings of IFToMM, Besancon, France*. Paper A-954. 2007.
[18] N., Dumitru, A., Margine. "Modeling bases in mechanical engineering". *Universitaria printing house. Craiova. Romania.* pp. 45-108. 2000.
[19] L. Gruionu, C. Bratianu, P. Rinderu, Numerical modelling and simulation in biomechanics. Universitaria Printing House Craiova. 2005.
[20] C-Y. E. Wang, J. E. Bobrow, Dynamic Motion Planning for the Design of Robotic Gait Rehabilitation J. of Biomech. Eng.127. 2005.
[21] C-Y. E., Wang, J. E. Bobrow and D. J. Reinkensmeyer, Swinging from the Hip: Use of Dynamic Motion Optimization in the Design of Robotic Gait Rehabilitation. IEEE Int. Conference on Robotics and Automation.2, pp. 1433–1438. 2001.
[22] K. Hashimoto, Y. Sugahara, A. Ohta, H. Sunazuka, Realization of Stable Biped Walking on Public Road with New Biped Foot System Adaptable to Uneven Terrain. BioRob 2006.
[23] D. Hooman, M. Brigitte Jolles, et. al., Estimation and Visualization of Sagittal Kinematics of Lower Limbs Orientation Using Body-Fixed Sensors. IEEE Transactions on Biomedical Engineering. Vol. 53. No.7 pp. 1385 – 1393. 2006.
[24] A., Heyn, R. E., Mayagoitia, A. V., Nene, and P. H., Veltink, "The kinematics of the swing phase obtained from accelerometer and gyroscope measurements". *Proceedings of the 18th Int. Conf. IEEE Engineering in Medicine and Biology Society*. pp. 463-464. 1996.
[25] S. Sameer, Intelligent Robotics For Rehabilitation Robotic Lower Limb for Above Knee Prosthesis. Grant type (83/ECE/2000) Department of Electronics and Communication Engineering India. 2004.
[26] A. Vucina, M. Hudec, Kinematics and forces in the above knee prosthesis during the stair climbing. Scientific paper MOSTAR Bosnia 2005.
[27] M. Williams, Biomechanics of human motion. W.B. Saunders Co. Philadelphia and London. 1996.